ISSN 0869-5911, Petrology, 2008, Vol. 16, No. 3, pp. 232–260. © Pleiades Publishing, Ltd., 2008.
Original Russian Text © P.Yu. Plechov, T.A. Shishkina, V.A. Ermakov, M.V. Portnyagin, 2008, published in Petrologiya, 2008, Vol. 16, No. 3, pp. 248–276.

Formation Conditions of Allivalites, Olivine–Anorthite Crystal Enclaves, in the Volcanics of the Kuril–Kamchatka Arc

P. Yu. Plechov[a], T. A. Shishkina[a], V. A. Ermakov[b], and M. V. Portnyagin[c, d]

[a] *Faculty of Geology, Moscow State University, Vorob'evy gory, Moscow, 119899 Russia*
e-mail: pavel@web.ru
[b] *Institute of Physics of the Earth, Russian Academy of Sciences, ul. Bol'shaya Gruzinskaya 10, Moscow, 123995 Russia*
[c] *Vernadsky Institute of Geochemistry and Analytical Chemistry, Russian Academy of Sciences, ul. Kosygina 19, Moscow, 119991 Russia*
[d] *Division of the Ocean Floor, IFM-GEOMAR, Wischhostr. 1–3, 24148 Kiel, Germany*

Received January 22, 2007; in final form May 27, 2007

Abstract—In this paper we address allivalites, coarse- and giant-textured olivine–anorthite rocks occurring as separate blocks in the eruption products of many volcanoes from the frontal part of the Kuril–Kamchatka arc. New data are reported on the petrography, mineralogy, and composition of melt inclusions in minerals from ten allivalite samples from Ksudach, Il'inskii, Zavaritskii, Kudryavyi, and Golovnin volcanoes. The crystallization temperatures of allivalite minerals were estimated as 970–1080°C at a melt water content of 3.0–3.5 wt % and oxygen fugacity NNO = 1–2. A genetic link was established between the compositions of melt inclusions and interstitial glasses in allivalites and volcano rocks. The cumulate nature of allivalites was demonstrated. Using mass balance calculations, the degree of fractionation of primary melts during the formation of cumulate layers was estimated for various volcanoes as 22–46%.

DOI: 10.1134/S0869591108030028

INTRODUCTION

Peculiar holocrystalline coarse- and giant-textured olivine–anorthite enclaves in extrusive rocks from many volcanoes of Kamchatka and the Kuril Islands have been known since the studies of B.I. Piip (e.g., Piip, 1947). The first petrographic description and analyses of minerals from these rocks were presented by Sheimovich (1966) and Dubik (1969). These enclaves were described under different names: gabbroid inclusions (Piip, 1947; Sheimovich, 1966; Dubik, 1969), olivine anorthosite (Selyangin, 1974), allivalite (Rodionova and Fedorchenko, 1971; Masurenkov, 1974), and olivine–anorthite rocks (Volynets et al., 1978). Enclaves of olivine–anorthite rocks proper associate with various pyroxene–olivine–plagioclase gabbroids, including eucrites, troctolites, amphibole gabbros, etc. This is probably why Bogoyavlenskaya and Erlikh (1969) described an olivine–pyroxene–anorthite enclave as an anorthositic microtinite (pyroxene was misidentified as glass).

Although the term allivalite (Harker, 1909) was proposed for the rocks described in the layered intrusion of the Isle of Rhum, Scotland, this name has been used in the literature for olivine–anorthite rocks, in particular, for crystalline enclaves in the volcanic rocks of Kamchatka. Allivalites differ from troctolites (e.g., Lundgaard et al., 2002) in that they (1) contain the assemblage of calcic plagioclase ($An > 90$) and iron-rich olivine ($Fo < 81$) and (2) show very small variations in mineral compositions within a single sample (by 2–3 in anorthite or forsterite number).

Allivalites were described in many volcanoes of Kamchatka: Kikhpinych, Ksudach, Kambal'nyi, Il'inskii, Zheltovskii, Koshelevskii, Mutnovskii, Malyi Semyachik, and Karymskii (Grib, 1997; Volynets et al., 1978 and references therein; Selyangin, 1980) and the Greater Kuril arc: Mendeleev, Kudryavyi, calderas of Golovnin, Nemo, and Zavaritskii (Masurenkov, 1974), Tao-Rusyr, and Ebeko (Dril', 1988). Similar rocks were reported from the outer zones of volcanic arcs of northern Japan: Miyakejima, Nekoma, Rishiri, and Akagi (Amma-Miyasaka and Nakagawa, 2002; Ishikawa, 1951). Large blocks of the gabbro–allivalite association, up to several hundred kilograms in weight, were found in the Lesser Antilles (Arculus and Willis, 1980).

All allivalites were reported from volcanoes of front-arc areas (Frolova et al., 2000; Amma-Miyasaka and Nakagawa, 2002), whose general feature is the presence of low-potassium island-arc tholeiites among the eruption products (Frolova et al., 2000). Allivalites occur mainly among tephras and volcanics of rhyolitic, rhyodacitic, and, occasionally, andesitic compositions (Volynets et al., 1978; Frolova et al., 2000), whereas the basalts contain glomerophyric intergrowths of olivine and plagioclase.

In addition to allivalites, the volcanics of the Kuril–Kamchatka arc contain enclaves of various anorthite-bearing gabbroids, which are referred to as the gabbro–

allivalite association (Ermakov and Pecherskii, 1989). For instance, amphibole–anorthite rocks chemically similar to allivalites were found in Avacha, Uspenskii, and Mount Ostraya volcanoes; in the Miocene andesites of Paramushir (described by V.A. Ermakov); and high-Al basalts of the Tatun Volcano group in northern Taiwan (Chen, 1978). The occurrence of gabbro–allivalites and their association with other types of crystalline enclaves from the volcanoes of the Kuril–Kamchatka arc were considered by Ermakov et al. (1987) and Ermakov and Pecherskii (1989). The scope of this paper is limited to allivalites.

The investigation of the compositions of melt inclusions in olivines and plagioclases from the allivalites of four volcanoes of the Kuril–Kamchatka island arc revealed a genetic link between allivalites and their host extrusive rocks, established the cumulate nature of allivalites, and allowed estimation of the temperature of simultaneous crystallization of the minerals of the olivine–plagioclase association as 1050–1100°C (Frolova et al., 2000). Frolova et al. (2000) supposed that allivalites could be formed by the fractionation of 7–8% olivine and anorthite from an initial water-rich (1.5–2.0 wt % H_2O) melt, whose evolution led to the formation of extrusive series of the respective volcanoes of Kamchatka and the Kuril Islands.

This paper reports a detailed description of the mineralogy of allivalites, their classification, and possible mechanisms of the formation of these rocks. New data were obtained by the investigation of melt inclusions in olivine from ten samples of allivalites of various morphological types from Ksudach, Il'inskii, Zavaritskii, Kudryavyi, and Golovnin volcanoes. New analyses were reported for the major minerals, homogenized melt inclusions, daughter mineral phases in crystallized melt inclusions, and groundmass glasses of allivalites. The obtained results were used to evaluate the existing hypotheses of allivalite formation, confirm their cumulate genesis, and estimate their formation conditions.

METHODS

Thermometric experiments with a visual control were carried out at the Vernadsky Institute of Geochemistry and Analytical Chemistry, Russian Academy of Sciences using a low-inertia microscopic heating stage designed by Sobolev and Slutsky (Sobolev et al., 1980). Standard procedures described by Portnyagin et al. (2005) were used.

Quenching experiments on the partial homogenization of inclusions (Danyushevsky et al., 2002a) were conducted at the laboratory of experimental petrography of Moscow State University in an electric furnace with SiC heating elements. Olivine grains, 0.5–1.0 mm in size, were loaded into ceramic crucibles together with graphite crumbs, which imposed external redox conditions at the level of the CCO buffer and prevented grain oxidation at high temperatures. The experiment duration was no longer than 10 min at temperatures higher than 1000°C in order to prevent significant water losses from melts in the inclusions. The samples were quenched at 1200°C in water. After quenching, grains containing melt inclusions no less than 20 μm in size were picked out and polished until the inclusions were exposed on the surface.

The compositions of minerals and melt inclusions from allivalites were determined using a Camscan-4DV electron microscope equipped with a LinkSystem-10000 energy-dispersive system (petrology chair, Moscow State University; analysts E.V. Guseva and N.N. Korotaeva) at an accelerating voltage of 15 kV. Mineral phases were analyzed with a focused electron beam (3×3 μm), and glasses from inclusions and groundmass were analyzed by scanning over an area of at least 10×12 μm. Images were recorded in a backscattered mode at an accelerating voltage of 20 kV.

The content of water in glasses was determined by secondary ion mass spectrometry using a Cameca-ims4f ion microprobe at the Institute of Microelectronics and Informatics, Russian Academy of Sciences (Yaroslavl). The analytical procedure was described by Sobolev (1996).

OBJECTS

The allivalite samples studied here were taken from the following volcanoes of the Kuril–Kamchatka island arc: Ksudach, Il'inskii (southern part of the Kamchatka Peninsula), Zavaritskii (Simushir I.), Kudryavyi within the Medvezh'ya caldera (northeastern part of Iturup I.), and Golovnin (southern end of Kunashir I.) (Fig. 1, Table 1). All of the volcanoes occur in a frontal position relative to the trench and have complex and prolonged histories, including the formation of calderas and post-caldera activity. Their extrusive rocks form a continuous series from basalt to dacite. Allivalite nodules usually occur in intermediate and silicic pyroclastic rocks, occasionally in lavas. Most allivalite finds are related to large caldera-forming eruptions (Volynets et al., 1978; Selyangin, 1987; Frolova et al., 1988, 1989).

Allivalite enclaves have often irregular (small-fragment, block, and flattened) and, occasionally, spherical shapes. The fragments vary in size from 1 cm to 0.5 m and are usually surrounded by a film of dark glassy material.

The structures of allivalites are diverse, including massive, banded, and taxitic ones. Banded and taxitic structures develop when the rock is separated into zones with different proportions of plagioclase and olivine and different grain-size characteristics.

The internal structure of allivalites is very diverse. Several main textural types can be distinguished. (1) Allivalites with cumulate-textured olivine and plagioclase are rather common (Ksudach, Il'inskii, Zavaritskii, and Golovnin volcanoes) (Figs. 2a, 2c, 2e). The samples often disintegrate, because they are composed

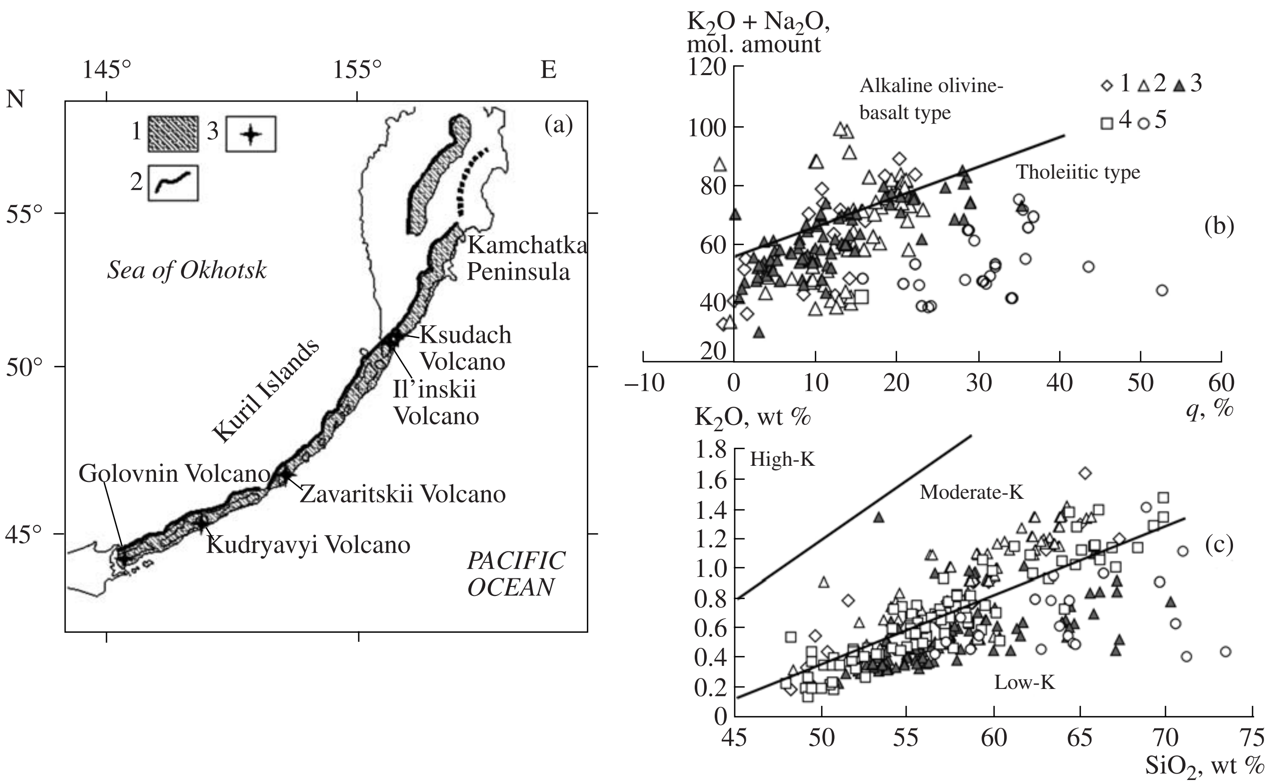

Fig. 1. (a) Area of occurrence of Recent low-potassium volcanics in the Kuril–Kamchatka island arc (Piskunov, 1976). (1) Area of occurrence of tholeiitic rocks, (2) line separating the rocks of tholeiitic and alkali olivine basalt types, and (3) volcanoes investigated in this study. Classification diagrams (b) ($K_2O + Na_2O$)–q (Piskunov, 1976) and (c) K_2O–SiO_2 for the petrochemical series of (1) Ksudach, (2) Il'inskii, (3) Zavaritskii, (4) Kudryavyi, and (5) Golovnin volcanoes. The parameter q reflects the excess (deficit) of silica necessary for the formation of the most saturated minerals: $q = 60[SiO_2 + TiO_2 + Fe_2O_3 - FeO - MnO - MgO - CaO - Al_2O_3 - 5(Na_2O + K_2O)]/1000$ (%), where oxides are in molar amounts (Piskunov, 1976).

of separate crystals varying in size from a few millimeters to 2–3 cm almost without a cementing groundmass. With respect to the size of olivine and plagioclase grains, the cumulate aggregates of allivalites can be subdivided into equigranular and porphyritic varieties. The interstices between the minerals and fractures in them are often filled with a partly crystallized brown volcanic glass containing plagioclase, pyroxene, and titanomagnetite microlites and rounded pores (Figs. 2i–2k). The glass is unevenly distributed in the enclaves. (2) Some enclaves (Kudryavyi Volcano) are concentrically zoned (Figs. 2b, 2d, 2f). Their central part is made up of large (2–5 mm) subhedral crystals of olivine and plagioclase. The outer zone is composed of large plagioclase grains (up to 1–2 mm in size) with randomly distributed small rounded olivine grains, up to 0.1 mm in diameter (Figs. 2d, 2f). Plagioclase and olivine sometimes form banded and reticulate intergrowths. (3) There are also porphyritic rocks with large (up to 10–15 mm) plagioclase and olivine phenocrysts in a fine-grained groundmass (Ksudach Volcano) (Volynets, 1978).

Frolova et al. (1989) reported evidence for melting in the marginal zones of allivalite blocks from Zavaritskii Volcano, including frosting on some pyroxene grains. We did not observe clear indications for the melting of allivalite minerals, but the concentrically zoned allivalites from Kudryavyi Volcano are surrounded by a cryptocrystalline rim zone, 2–5 mm wide, which contains small crystals of clinopyroxene and magnetite and large (up to 2–3 mm) zoned phenocrysts of plagioclase (64–74% *An*) (Fig. 2l). In general, the rim around the allivalites has an andesitic composition (63 wt % SiO_2, see below) (Table 4).

MINERALOGY OF ALLIVALITES

The major minerals of allivalites are plagioclase (An_{88-97}) and olivine (Fo_{69-81}); clinopyroxene and titanomagnetite were observed in some samples. Minor amounts of orthopyroxene and amphibole may be present (Ksudach and Il'inskii volcanoes). Partly crystallized brownish glass is common. It fills voids between the minerals and fractures in them. The proportions of minerals vary considerably among samples from a single volcano. Plagioclase is usually the most abundant mineral.

Table 1. Compositions of olivine and plagioclase from the allivalite samples

Volcano	Sample no.	Range of olivine composition, *Fo* mol %	Average composition of olivine, *Fo* mol % ± standard deviation	Range of plagioclase composition, *An* mol %	Average composition of plagioclase, *An* mol % ± standard deviation
Ksudach	Ks-1	74.8–75.9 (21)	75.5 ± 0.3	92.0–93.8 (7)	92.9 ± 0.7
	Ksud-2	78.7–79.9 (16)	79.5 ± 0.5	94.3–96.4 (13)	95.3 ± 0.6
	Ks-3	79.7–80.8 (20)	80.4 ± 0.3	92.5–94.6 (10)	93.7 ± 0.7
Il'inskii	Si-5	78.6–78.9 (2)	78.7 ± 0.2	88.0–91.4 (9)	89.6 ± 1.2
Zavaritskii	C-305/7	77.8–79.7 (22)	78.8 ± 0.5	93.4–95.8 (10)	94.4 ± 0.9
Kudryavyi	Kudr-1	77.0–79.0 (8)	78.3 ± 0.7	93.8–96.0 (10)	95.0 ± 0.7
	Kudr-E-03	78.7–80.1 (12)	79.6 ± 0.5	92.2–95.2 (7)	94.1 ± 1.2
Golovnin	115a	75,0–76.5 (12)	75.8 ± 0.5	95.5–97.0 (2)	96.2 ± 0.4
	6636/gp-15	69.2–71.1 (10)	69.9 ± 0.5	93.6–96.1 (12)	94.4 ± 0.7
	6636/gp-18	77.7–79.5 (9)	78.5 ± 0.6	95.4–97.1 (14)	96.2 ± 0.4

Note: Numbers of analyses are given in parentheses next to the ranges of mineral compositions.

Plagioclase

Plagioclase accounts for 50–90% of the rocks and forms isometric, tabular, or, occasionally, anhedral grains ranging from a few millimeters to a few centimeters in size. Glomerocrystalline clots of large plagioclase or plagioclase and olivine grains are widespread. Large plagioclase phenocrysts often contain small rounded olivine inclusions (Figs. 2g, 2h). Olivine phenocrysts contain small crystalline inclusions of plagioclase, whose composition is identical to the composition of plagioclase phenocrysts from the same sample (Fig. 6).

Despite the complex structure of allivalites, the composition of plagioclase from a single sample is almost constant (anorthite number varies by 1–3) (Table 1). The plagioclases of allivalites are unzoned, and their composition corresponds to anorthite ($An_{88–97}$) (Tables 1, 2; Fig. 3a). In contrast, plagioclase phenocrysts from the host volcanics (basalts and andesites) are distinctly zoned. For instance, plagioclase phenocrysts from the basalts of Golovnin Volcano have compositions of $An_{69–95}$.

The plagioclase grains show polysynthetic twinning; there are bending and displacement of twins and block extinction of grains, which may indicate mechanical stresses after the crystallization. Small gas inclusions and inclusions of dark-colored minerals were observed along cleavage surfaces.

Olivine

Olivine forms isometric or rounded subhedral grains, from 0.2 mm to several millimeters or even centimeters in size, and its content in the rocks ranges from a few percent to 35–40%. It occurs as individual grains, glomerocrystalline clots with plagioclase and clinopyroxene, and small rounded inclusions in plagioclase. Some olivine grains contain inclusions of magnetite and, very rarely, chrome spinel. Olivine from sample Kudr-E-03 contains small (20–50 μm) rounded inclusions of clinopyroxene ($En_{39–44}Fs_{10–14}Wol_{46–48}$) and plagioclase ($An_{92–95}$).

Olivine grains from allivalites are not zoned. Within any sample, the forsterite number of olivine varies within 1–3, but olivine composition may be significantly different between samples from a single volcano (Tables 1, 2; Fig. 3a). The most common olivine composition is $Fo_{78–81}$, although more fayalitic olivines (up to Fo_{69}) were detected in some samples (Ksudach and Golovnin volcanoes).

Clinopyroxene

Clinopyroxene occurs in amounts up to 10 vol % in the allivalites and forms anhedral grains, up to several millimeters in size. The grain boundaries are rugged and resorbed. The clinopyroxene is pleochroic in green shades in thin sections. Clinopyroxene in samples from different volcanoes shows different compositions: $En_{43–44}Fs_{12–13}Wo_{44–45}$ in Golovnin Volcano, $En_{32–34}Fs_{22–23}Wo_{41–46}$ in Kudryavyi Volcano, and $En_{42–44}Fs_{11–12}Wo_{45–46}$ in Ksudach Volcano (Table 2, Fig. 4).

Orthopyroxene

Orthopyroxene occurs as individual grains in some allivalite samples. Its composition in the allivalites of Golovnin Volcano ($En_{72}Fs_{26}Wo_3$) is similar to that of phenocrysts from the host basalt ($En_{64–69}Fs_{27–33}Wo_{3–4}$) (Tables 2, 3).

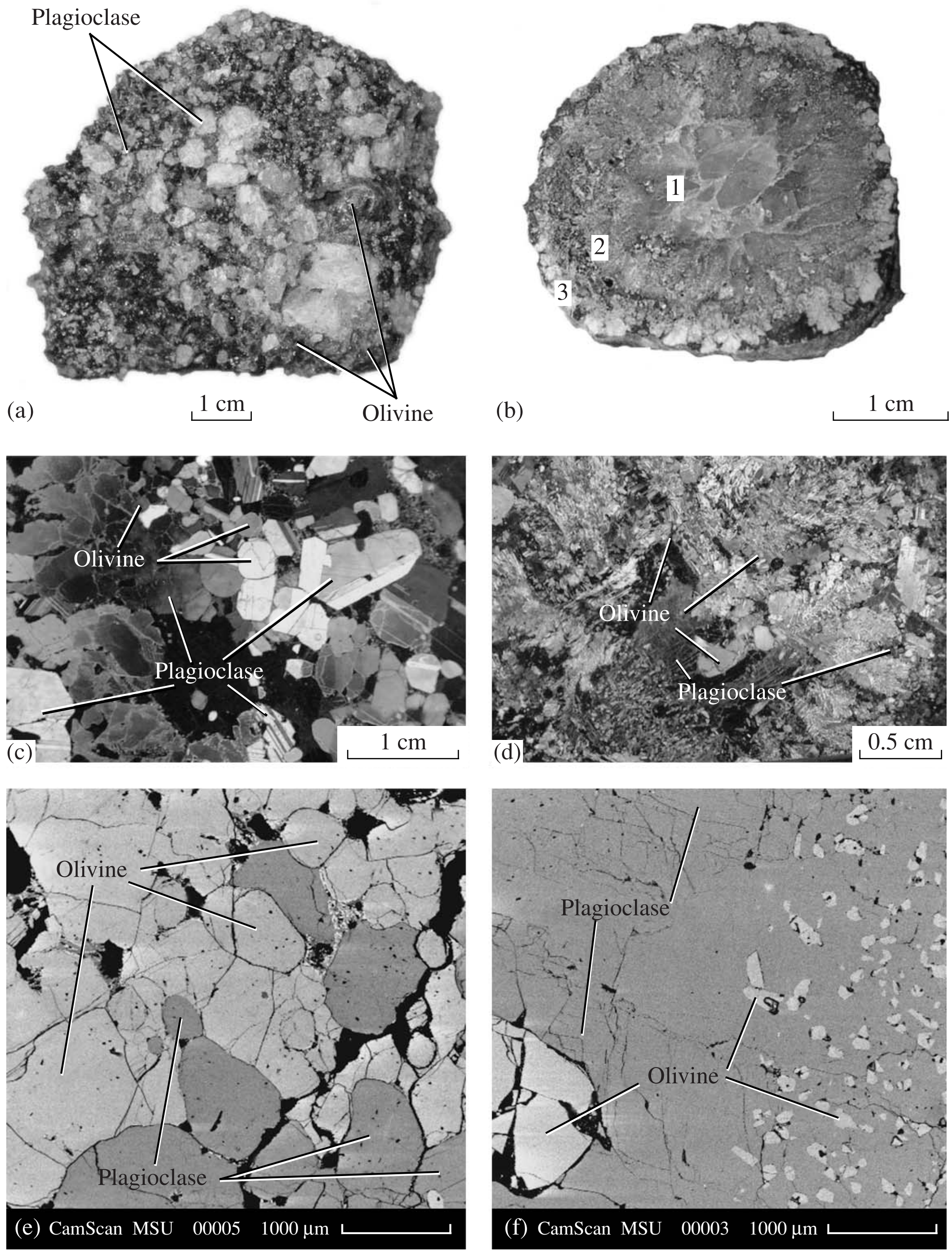

Fig. 2. Textural and structural features of allivalites. (a) Allivalite enclave (sample Ksud-2 from Ksudach Volcano) with plagioclase and olivine crystals forming a cumulate porphyritic texture. (b) Concentrically zones allivalite enclave (sample Kudr-1, Kudryavyi Volcano): 1—zone of pegmatoid plagioclase, 2—zone of closely intergrown olivine and plagioclase, and 3—zone of thermal alteration. (c) Allivalite (sample Ks-1, Ksudach Volcano) in cross-polarized light, magnification ×2.5. (d) Concentrically zoned allivalite enclave (sample Kudr-1, Kudryavyi Volcano) consisting of large euhedral olivine and plagioclase crystals in the center and a rim of intergrown olivine and plagioclase; cross-polarized light. (e) Back-scattered electron image of allivalite (sample Ks-1, Ksudach Volcano). (f) Back-scattered electron image of allivalite (sample Kudr-1, Kudryavyi Volcano) exhibiting a transition from the coarse-grained zone to the zone of close intergrowth of olivine and plagioclase. (g) Rounded inclusion of olivine in plagioclase (sample 115a, Golovnin Volcano); cross-polarized light. (h) Rounded inclusions of olivine in large plagioclase grains (sample 6636/gp-15, Golovnin Volcano); cross-polarized light. (i) Back-scattered electron image of crystallized interstitial glass (sample Ksud-2, Ksudach Volcano). (j) Back-scattered electron image of an allivalite fragment (sample Kudr-1, Kudryavyi Volcano) with partly crystallized glass. (k) Back-scattered electron image of crystallized glass between olivine grains (sample 115a, Golovnin Volcano). (l) Plagioclase phenocryst replaced by a cryptocrystalline aggregate with 90–95 wt % SiO_2 and surrounded by a fine-grained material of andesitic composition from a mantle around allivalite (sample Kudr-E-03, Kudryavyi Volcano).

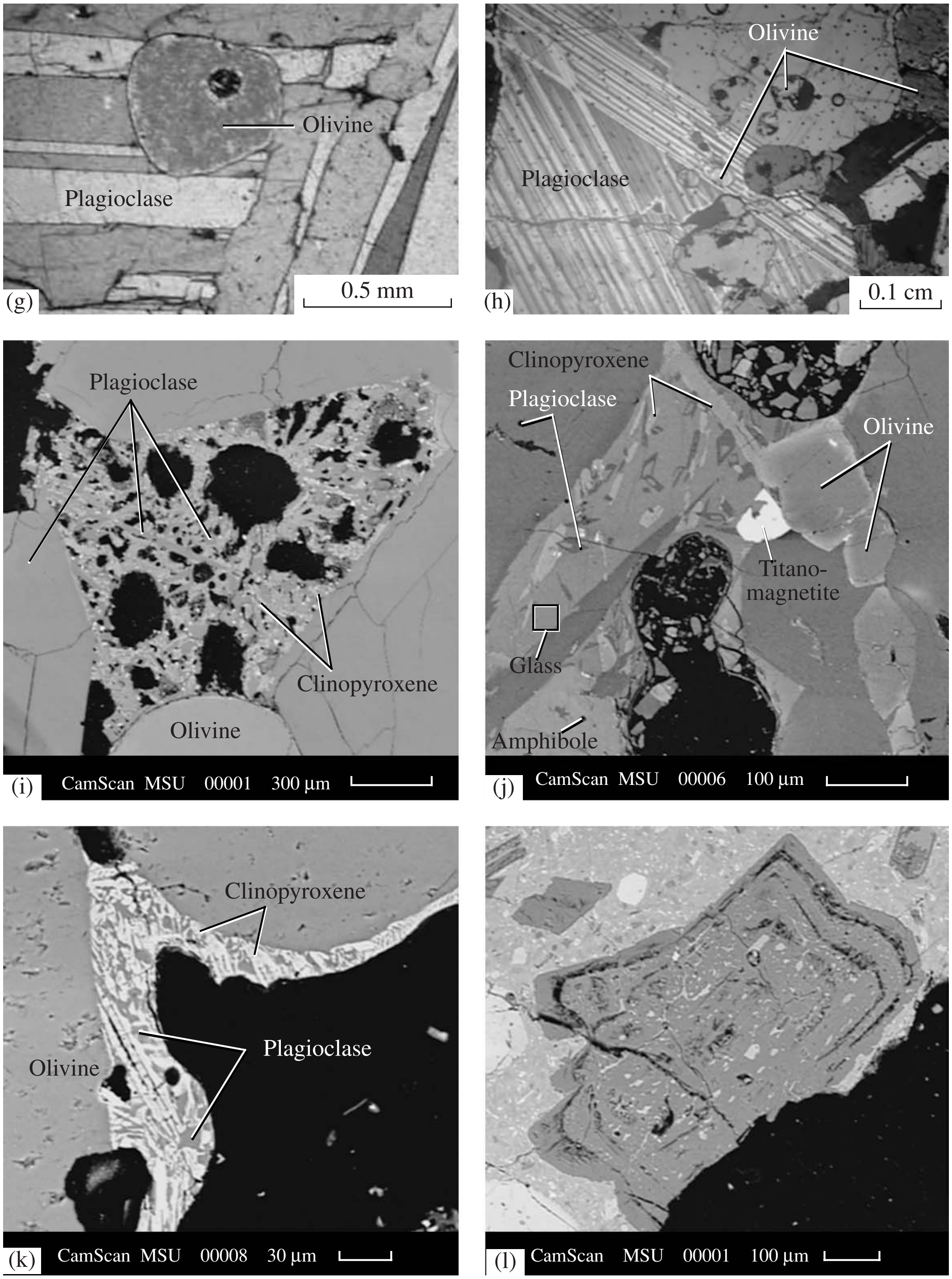

Fig. 2. (Contd.).

Titanomagnetite

Minor amounts of titanomagnetite were found in allivalites. It forms individual isometric or angular grains, up to 100 μm in size, and often occurs as inclusions in olivine and clinopyroxene. The compositions of titanomagnetite are shown in Table 2. There is no evidence for the unmixing of the titanomagnetite solid solution.

Chrome Spinel

Chrome spinel is not a characteristic mineral of allivalites, in contrast to the basalts of the same volca-

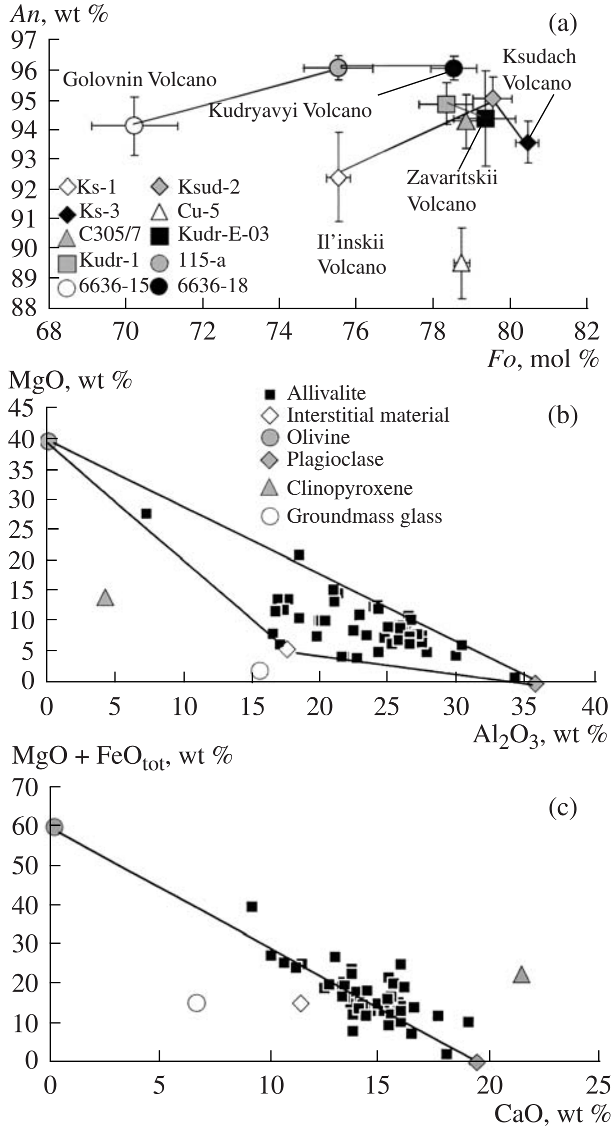

Fig. 3. (a) Compositional ranges of olivine (*Fo*, mol %) and plagioclase (*An*, mol %) for particular allivalite samples from the Kuril–Kamchatka island arc. The symbols correspond to arithmetic mean values. Samples from a single volcano are connected by lines. (b) and (c) Compositions of allivalites after Bogoyavlenskaya and Erlikh (1969), Volynets et al. (1978), Dril' (1988), Selyangin (1974), Frolova et al. (2000), and Sheimovich (1966) and average compositions of minerals and interstitial materials from the allivalite samples studied by us.

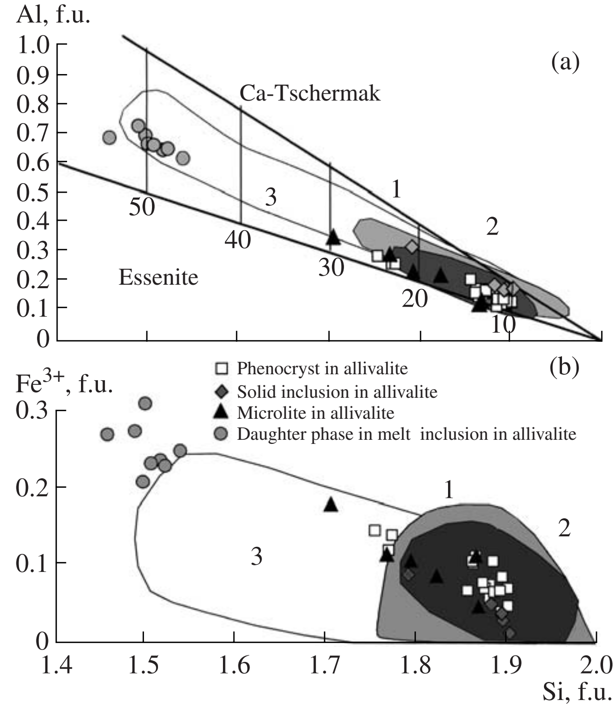

Fig. 4. Compositions of clinopyroxene from allivalites. (a) Total Al content as a function of Si. (b) Contents of Fe^{3+} calculated from the stoichiometry as a function of Si. Fields of clinopyroxene compositions from various volcanics of Kamchatka (our data): 1, phenocrysts; 2, microlites; and 3, solid inclusions and daughter phases in melt inclusions. The compositions are given in atomic formula units (f.u.) calculated for 6 oxygen atoms.

noes. Prikhod'ko et al. (1977) reported a finding of chrome spinel in allivalites from Ksudach Volcano. We observed rare inclusions of chrome spinel in olivine grains from samples Ks-3 (Ksudach Volcano) and 6636/gp-18 (Golovnin Volcano) and much more abundant chrome spinel in olivine of the same fayalite number from the basalts of Golovnin Volcano (samples 116a and 6636/gp-5). Chrome spinel occurs as isometric crystals, 20–50 μm in size, sometimes surrounded by thin melt films (Figs. 5a, 5b). Oxygen fugacity was calculated on the basis of the olivine–chrome spinel equilibrium (Ballhaus et al., 1991) (Fig. 5c). The f_{O_2} values of both the basalts and allivalites appeared to correspond to oxidizing conditions between NNO + 1 and NNO + 2. The compositions of chrome spinel from the allivalites and basalts are given in Tables 2 and 3, respectively.

Volcanic Glass

Brown glass fills interstices between minerals and microscopic fractures in rocks and sometimes forms crusts around individual nodules (Kudryavyi Volcano). It has a vesicular, slaglike, or massive structure (Figs. 2i–2k) and is mostly crystallized to skeletal, dendritic, and isometric crystals of plagioclase, clinopyroxene, and magnetite cemented by a small amount of glass. The compositions of microlites from the glass are significantly different from those of major minerals in allivalites (Table 4). Plagioclase in the glass is much more sodic than plagioclase phenocrysts, its composition corresponds to labradorite–bytownite ($An_{58–77}$) and contains more iron (0.9–1.85 wt %) than plagioclase from allivalites (0.4–0.9 wt %) (Fig. 6).

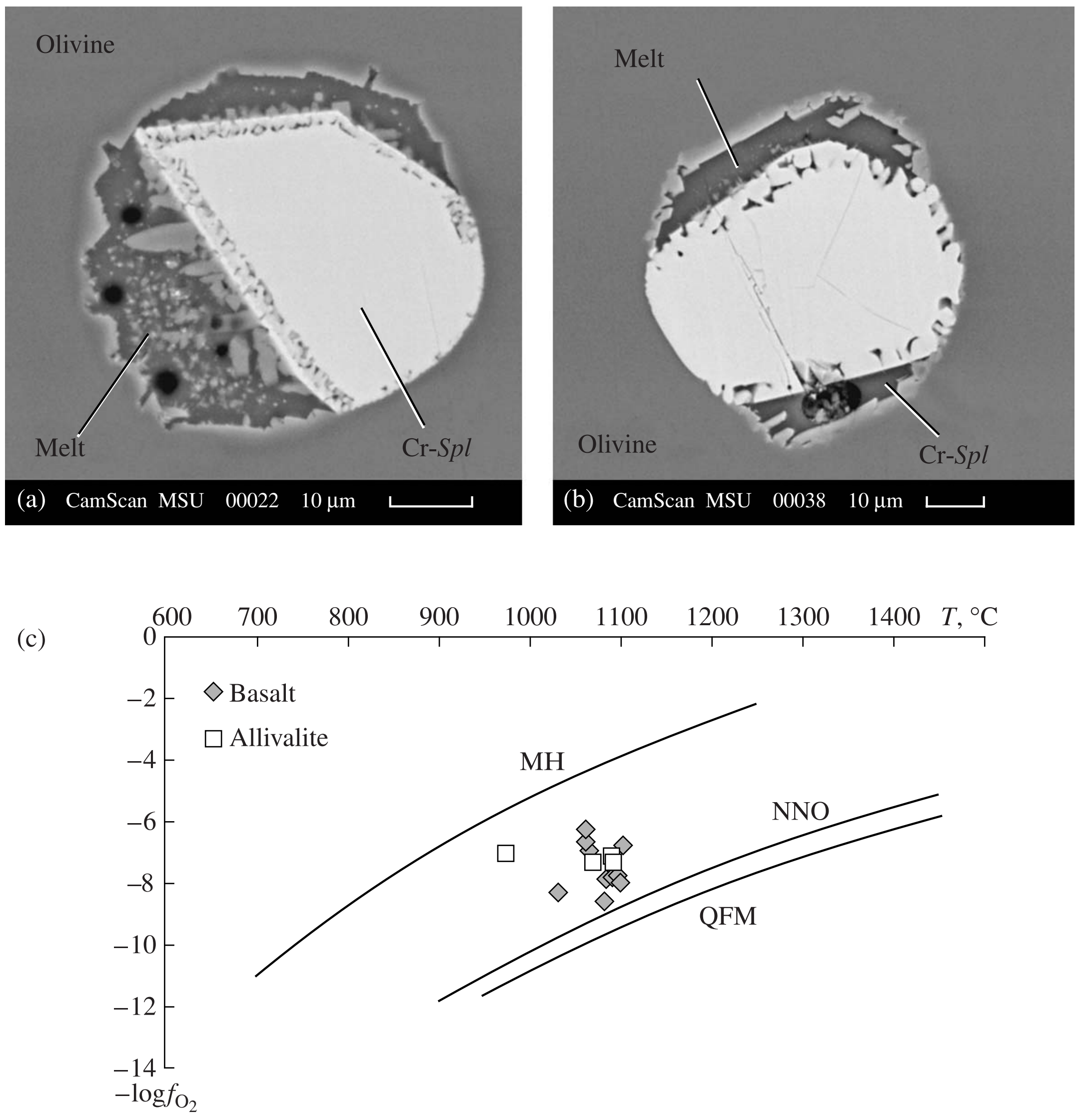

Fig. 5. Solid inclusions of chrome spinel in olivine from (a) the allivalite of Golovnin Volcano and (b) the basalt of Golovnin Volcano. (c) Oxygen fugacity estimated on the basis of chrome spinel–melt equilibrium (Ballhaus et al., 1991).

The groundmass of allivalite from the Golovnin Volcano is completely crystallized (Fig. 2k). The main minerals are subcalcic clinopyroxene and plagioclase (Table 4).

Partly crystallized glass occurs in the central parts of allivalite nodules from Kudryavyi Volcano in the interstices between minerals. It contains skeletal crystals of clinopyroxene and plagioclase and residual glass (Table 4).

MELT INCLUSIONS AND THEIR DAUGHTER PHASES

The abundance of melt inclusions in the minerals of allivalites was mentioned by many authors (Selyangin, 1975; Anan'ev and Shnyrev, 1984; Frolova et al., 2000). Melt inclusions were found in all major minerals of allivalites. Glassy inclusions occur in plagioclase grains as tiny droplets along cleavage fractures. In clinopyroxene grains, inclusions are rare; they have rounded shapes and sizes of 10–30 μm.

All primary melt inclusions in olivine are nearly spherical in shape and are partly crystallized. They appear as dark hairy clots in transmitted light. The back-scattered electron images of representative melt inclusions from sample C-305/7 are shown in Fig. 7. Residual glass occurs in all of the inclusions.

Daughter Minerals in Melt Inclusions

With respect to the association of daughter phases, the inclusions can be subdivided into several types. The inclusions of the first type (Fig. 7a) contain daughter clinopyroxene, which rims the inclusion walls and

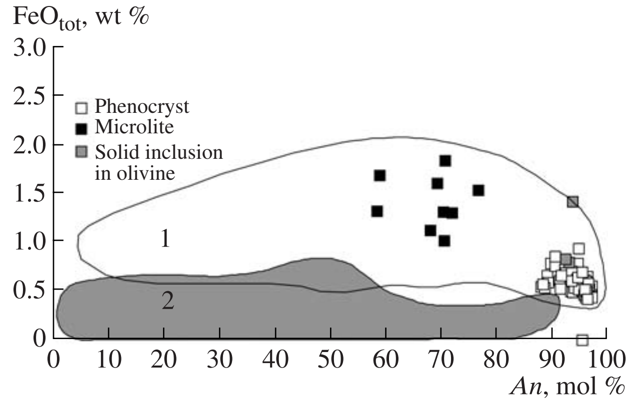

Fig. 6. Compositions of plagioclase from allivalites. (*1*) Field of plagioclases from the volcanic rocks of Kamchatka (our data) and Japan (Amma-Miyasaka and Nakagawa, 2002) and (*2*) field of plagioclasees from high-temperature eclogite and granulite complexes (V.O. Yapaskurt, Moscow State University (MSU) unpublished data).

forms spear-shaped crystals within the inclusions. The inclusions of the second type (Fig. 7b) contain dendritic daughter crystals of amphibole. The daughter phase of inclusions of the third type is represented by plagioclase microlites (Fig. 7c) cemented by amphibole dendrites and glass. We observed inclusions transitional between the first and second types; they contain clinopyroxene crystallizing on the walls and dendritic amphibole overgrowing the clinopyroxene.

The average compositions of daughter phases are given in Table 5. The clinopyroxene is extremely depleted in silica (up to 37.5 wt % SiO_2) and enriched in aluminum, iron, and titanium at the expense of Tschermak end-members. Anan'ev and Shnyrev (1984) misinterpreted this clinopyroxene as garnet on the basis of microprobe analyses only. The mineral forms wedge-shaped crystals and displays birefringence and oblique extinction. The high contents of Ca-Tschermak and essenite components are characteristic of daughter clinopyroxene crystals in inclusions in olivine (Portnyagin et al., 2005) and related to the metastable conditions of clinopyroxene growth within the inclusions, while plagioclase nucleation was suppressed. Figure 4 compares the compositions of daughter clinopyroxenes from melt inclusions in olivine from the volcanic rocks of Kamchatka with those of clinopyroxene phenocrysts and microlites. The compositions of all clinopyroxenes from allivalites form a regular sequence, with daughter clinopyroxenes at one extreme with up to 54% of the Ca-Tschermak end-member. Similar clinopyroxene compositions with 52–54% of the Ca-Tschermak component were reported from experiments (Sack and Carmichael, 1984; Gee and Sack, 1988). We believe that such high contents of the Ca-Tschermak component in experiments also reflect the metastable conditions of clinopyroxene crystallization.

Another characteristic daughter mineral in melt inclusions from allivalites is amphibole. It forms dendrite-like and fanlike intergrowths sometimes overgrowing clinopyroxene. We described several inclusions containing both plagioclase and amphibole (Fig. 7c), and plagioclase crystallized in them before amphibole. Perhaps, conditions favorable for amphibole crystallization in the inclusions developed owing to water enrichment during crystallization, which, on the one hand, suppresses plagioclase crystallization (Pletchov and Gerya, 1998) and, on the other hand, promotes the appearance of amphibole as a hydrous mineral. Thus, the presence of amphibole in partly crystallized inclusions indicates high water contents in their melts.

Similar to the daughter clinopyroxene crystals, the daughter amphibole is rich in Al_2O_3 and CaO and contains significant amounts of Na_2O and K_2O. According to the IMA classification (Leake et al., 1997), the compositions of these amphiboles correspond to the tschermakite–pargasite series (Table 5). It is usually thought that the tschermakite component in amphibole is indicative of high pressures (Anderson and Smith, 1995), but in the case considered, the high tschermakite content of amphibole was due to its metastable crystallization rather than high pressures, which is similar to the daughter clinopyroxenes described above.

Method of Reconstructing the Compositions of Initial Allivalite Melts

The compositions of initial melts for the allivalites were estimated on the basis of the analyses of melt inclusions in olivine (Table 6). For this purpose, we used homogenized primary melt inclusions, no smaller than 20 μm in size and without indications for decrepitation and oxidation (Fig. 7d).

The melt inclusions were experimentally heated to the temperatures of the complete melting of daughter phases. These temperatures may be both lower and higher than the real temperatures under which the inclusions were trapped, which resulted in significant variations in the amount of olivine removed from the inclusion walls during the experiments and deviations of the compositions of the quenched inclusions from those of the initial melts. In particular, this is suggested by the considerable scatter of FeO_{tot} in the inclusions (10–18 wt %), which is much higher than the FeO_{tot} variations in the basalts of the Kuril Islands and Kamchatka. Therefore, the measured compositions of inclusions reflect local melt–olivine equilibrium at the inclusion boundary under experimental temperatures and cannot be directly interpreted as the compositions of the initial melts that produced the allivalite mineral assemblage.

The interpretation of the compositions of experimentally quenched melt inclusions is a common problem in petrological investigations (e.g., Danyushevsky

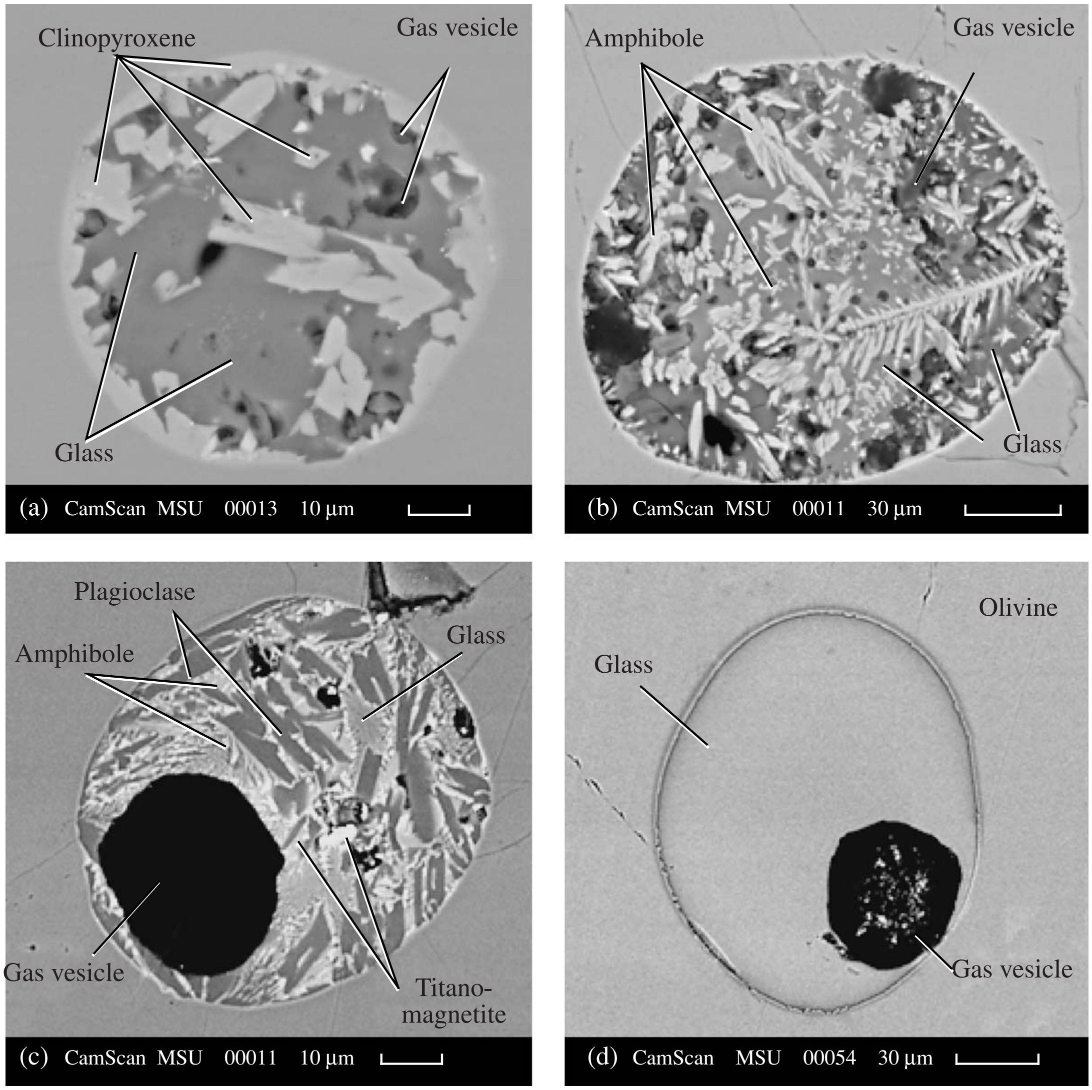

Fig. 7. Melt inclusions in olivine from allivalites. (a)–(c) Partly crystallized inclusions consisting of (a) clinopyroxene and glass; (b) amphibole and glass; and (c) plagioclase, amphibole, titanomagnetite, and glass. (d) Partly homogenized inclusion after a thermometric experiment.

et al., 2000; Portnyagin et al., 2005). In order to reconstruct melt compositions, Danyushevsky et al. (2000) proposed a method based on the numerical modeling of equilibrium between trapped melt and host olivine and independent estimation of the initial content of FeO in the inclusions from rock compositions (Danyushevsky et al., 2000) or modeling diffusion zoning in olivine around the inclusions (Danyushevsky et al., 2002b; Portnyagin et al., 2005). The contents of FeO_{tot} in allivalites cannot be considered identical to those in the initial compositions of inclusions, because the bulk compositions of allivalites are controlled mainly by the proportions of plagioclase and olivine in the cumulate and do not correspond to melt compositions (Figs. 3b, 3c). The alternative approach of modeling diffusion zoning is also inapplicable to inclusions in allivalites, because they do not show a loss of FeO_{tot} related to reequilibration with olivine but gain FeO_{tot} owing to the melting of excess olivine during the experiment. Thus, both the methods are not appropriate for the inclusions considered in this study.

We propose a method for the estimation of the composition of melt inclusions by postulating simultaneous olivine and plagioclase crystallization during melt entrapment and independently determining H_2O content in the inclusions.

The composition of an inclusion recalculated to equilibrium with the host olivine must satisfy the requirement of its equilibrium with plagioclase at the same temperature. Figure 8a shows by the example of the average compositions of melt inclusions from sample Ks-3 that the requirement of cotectic equilibrium with olivine and plagioclase can be satisfied in a dry system (0 wt % H_2O) only for a composition with the

Table 2. Compositions of major rock-forming minerals from allivalites, wt %

Sample no.	SiO_2	TiO_2	Al_2O_3	FeO_{tot}	MnO	MgO	CaO	Na_2O	K_2O	Cr_2O_3	NiO	Total	Mg# or *An* mol %
						Olivine							
Ks-1 (21)	38.45 (0.22)	–	–	21.79 (0.27)	0.50 (0.07	37.67 (0.21)	0.20 (0.07)	–	–	–	–	98.66	75.5 (0.3)
Ksud-2 (16)	38.20 (0.27)	–	–	19.25 (0.28)	0.31 (0.06)	41.90 (0.65)	0.21 (0.04)	–	–	–	–	99.97	79.05 (0.5)
Ks-3 (20)	39.26 (0.17)	–	–	17.81 (0.24)	0.39 (0.08)	40.89 (0.21)	0.20 (0.04)	–	–	–	–	98.60	80.4 (0.3)
Si-5 (2)	38.78 (0.03)	–	–	19.28 (0.09)	0.37 (0.13)	40.01 (0.28)	0.18 (0.08)	–	–	–	–	98.62	78.7 (0.2)
C-305/7 (22)	38.46 (0.32)	–	–	19.59 (0.52)	0.34 (0.1)	40.88 (0.32)	0.16 (0.04)	–	–	–	–	99.56	78.8 (0.5)
Kudr-1 (8)	39.07 (0.16)	–	–	19.44 (0.56)	0.48 (0.13)	39.47 (0.42)	0.19 (0.04)	–	–	–	–	98.70	78.3 (0.7)
Kudr-E-03 (12)	38.57 (0.33)	–	–	19.00 (0.35)	0.29 (0.08)	41.61 (0.48)	0.21 (0.04)	–	–	–	–	99.76	79.6 (0.5)
115a (12)	38.31 (0.38)	–	–	21.84 (0.69)	0.37 (0.11)	38.35 (0.47)	0.16 (0.04)	–	–	–	–	99.14	75.8 (0.5)
6636/gp-15 (10)	37.35 (0.32)	–	–	26.45 (0.65)	0.55 (0.20)	34.54 (0.57)	0.14 (0.05)	–	–	–	–	99.07	69.9 (0.5)
6636/gp-18 (9)	38.73 (0.34)	–	–	19.66 (0.49)	0.33 (0.17)	40.22 (0.8)	0.17 (0.05)	–	–	–	–	99.19	78.5 (0.6)
						Plagioclase							
Ks-1 (7)	43.94 (0.41)	–	35.38 (0.42)	0.72 (0.03)	–	–	19.08 (0.11)	0.81 (0.08)	–	–	–	99.95	92.9 (0.7)
Ksud-2 (13)	43.71 (0.47)	–	35.76 (0.47)	0.54 (0.16)	–	–	19.47 (0.18)	0.55 (0.08)	–	–	–	100.03	95.2 (0.7)
Ks-3 (10)	43.74 (0.32)	–	35.68 (0.2)	0.68 (0.04)	–	–	19.35 (0.2)	0.72 (0.08)	–	–	–	100.17	93.7 (0.7)
Si-5 (9)	44.97 (0.31)	–	35.11 (0.25)	0.57 (0.05)	–	–	18.46 (0.23)	1.18 (0.15)	–	–	–	100.30	89.6 (1.2)
C-305/7 (10)	43.69 (0.42)	–	35.95 (0.39)	0.53 (0.03)	–	–	19.54 (0.15)	0.64 (0.1)	–	–	–	100.36	94.4 (0.9)
Kudr-1 (10)	43.46 (0.33)	–	36.04 (0.31)	0.59 (0.05)	–	–	19.64 (0.14)	0.57 (0.08)	–	–	–	100.31	95.0 (0.7)
Kudr-E-03 (7)	44.59 (0.27)	–	34.46 (0.18)	0.70 (0.14)	–	–	19.23 (0.27)	0.67 (0.14)	–	–	–	99.66	94.1 (1.2)
115a (12)	43.40 (0.33)	–	36.12 (0.42)	0.55 (0.05)	–	–	19.84 (0.23)	0.43 (0.05)	–	–	–	100.28	96.2 (0.4)
6636/gp-15 (12)	43.93 (0.40)	–	35.67 (0.67)	0.61 (0.06)	–	–	19.54 (0.32)	0.63 (0.08)	–	–	–	100.40	94.4 (0.7)
6636/gp-18 (14)	43.38 (0.47)	–	36.13 (0.76)	0.50 (0.07)	–	–	19.96 (0.19)	0.43 (0.05)	–	–	–	100.41	96.2 (0.4)
						Clinopyroxene							
Ksud-2 (4)	50.85 (0.49)	0.45 (0.11)	3.49 (0.38)	7.02 (0.23)	0.24 (0.10)	15.12 (0.47)	22.24 (0.19)	0.20 (0.13)	–	–	–	99.79	79.3 (1.0)
Kudr-E-03 (3)	46.62 (0.33)	1.55 (0.17)	6.04 (0.36)	13.20 (0.52)	0.24 (0.12)	11.50 (0.79)	20.21 (1.06)	0.31 (0.12)	–	–	–	99.84	60.6 (0.7)
6636/gp-15 (2)	51.05 (0.31)	0.35 (0.10)	3.10 (0.18)	7.66 (0.57)	0.17 (0.04)	15.31 (0.34)	21.71 (0.28)	0.14 (0.18)	–	–	–	99.84	78.1 (1.7)
						Orthopyroxene							
6636/gp-15 (1)	53.43	0.22	1.24	16.85	0.44	26.33	1.34	0.07	–	–	–	99.92	73.6
						Titanomagnetite							
Kudr-E-03 (1)	–	7.71	4.03	84.84	0.15	2.06	–	–	–	0.01	0.35	99.69	
6636/gp-15 (2)	–	7.61 (0.04)	4.90 (0.03)	82.97 (0.40)	0.24 (0.05)	3.20 (0.02)	–	–	–	0.61 (0.21)		99.53	
						Chrome spinel							
Ks-1 (2)	–	2.03 (0.48)	34.53 (2.05)	39.89 (2.23)	0.22 (0.11)	12.11 (0.36)	–	–	–	10.98 (0.37)		99.91	
6636/gp-18 (1)	–	1.34	24.52	47.35	0.43	9.31	–	–	–	16.43		99.77	

Note: Here and in Tables 3 and 5, one standard deviation is shown in parentheses next to the content. Dashes mean that the content is below the detection limit. The numbers of mineral analyses is given in parentheses next to the sample name in the first column. Mg# is the Mg number of olivine and pyroxenes, and *An* is the mole fraction of the anorthite component in plagioclase. Sampling sites are given in Table 1.

Table 3. Compositions of phenocrysts from the basalts of Golovnin Volcano, wt %

Sample no.	SiO_2	TiO_2	Al_2O_3	FeO_{tot}	MnO	MgO
			Olivine			
116/1g (54)	38.68 (0.93)	–	–	20.39 (4.05)	0.30 (0.11)	39.99 (3.27)
6636/gp-5 (9)	38.73 (0.28)	–	–	20.17 (0.62)	0.41 (0.06)	39.01 (0.49)
			Plagioclase			
116/1g (8)	47.0 (3.89)	–	32.43 (3.10)	1.00 (0.59)	–	0.10 (0.09)
			Clinopyroxene			
6636/gp-5 (1)	52.34	0.15	2.42	6.32	0.31	15.68
			Orthopyroxene			
116/1g (3)	52.07 (1.31)	0.20 (0.07)	1.16 (0.27)	21.95 (5.09)	0.51 (0.13)	20.94 (5.16)
			Chrome spinel			
116/1g (5)	–	1.10 (0.83)	28.41 (2.98)	36.86 (5.62)	0.14 (0.07)	10.91 (1.40)
6636/gp-5 (3)	–	4.04 (1.6)	13.13 (2.63)	64.68 (8.13)	0.31 (0.30)	6.68 (0.86)

Sample no.	CaO	Na_2O	K_2O	Cr_2O_3	NiO	Total	Mg# or *An* mol %
			Olivine				
116/1g (54)	0.19 (0.06)	0.11 (0.09)	0.02 (0.02)	–	–	99.87 (0.08)	77.7 (5.0)
6636/gp-5 (9)	0.15 (0.03)	0.25 (0.10)	0.02 (0.02)	–	–	98.81 (0.10)	77.5 (0.8)
			Plagioclase				
116/1g (8)	17.25 (3.26)	1.74 (1.70)	0.09 (0.06)	–	–	99.84 (0.06)	84.4 (15.3)
			Clinopyroxene				
6636/gp-5 (1)	22.14	0.37	–	0.26	–	99.99	81.6
			Orthopyroxene				
116/1g (3)	2.74 (1.62)	0.12 (0.05)	0.02 (0.02)	–	–	99.82 (0.04)	62.4 (11.6)
			Chrome spinel				
116/1g (5)	0.05 (0.02)	0.10 (0.12)	0.02 (0.03)	21.98 (2.78)	0.12 (0.04)	99.83 (0.09)	
6636/gp-5 (3)	0.09 (0.08)	0.21 (0.05)	0.01 (0.02)	9.01 (6.62)	–	98.31 (0.42)	

initial FeO_{tot} = 13.5 wt %. The presence of H_2O exerts a stronger influence on the liquidus temperature of plagioclase than olivine (e.g., Danyushevsky et al., 2002b), and the cotectic composition is shifted in hydrous melts toward plagioclase, i.e., to lower FeO and MgO contents (Fig. 8b). If the melt H_2O content is known, the cotectic composition and equilibrium temperature can be unambiguously determined (Fig. 8c). Thus, the proposed approach provides a means to reconstruct the initial composition of melt inclusions in olivine and crystallization conditions at known melt H_2O contents, if the simultaneous crystallization of olivine and plagioclase during the inclusion entrapment is demonstrated. The accuracy of the method is limited only by the adequacy of existing numerical models for the description of olivine–plagioclase–melt equilibrium in the presence of variable amounts of H_2O (Fig. 8).

The presence of cumulate textures formed mainly by olivine and plagioclase and inclusions of one mineral in the other provide compelling evidence for the cocrystallization of plagioclase and olivine during allivalite formation (Fig. 2). The measured maximum H_2O contents in the inclusions from various samples are stable (3.0–3.5 wt %; Table 6) and probably close to the initial contents during the entrapment of these inclusions. Thus, both the requirements necessary for the application of our method are satisfied in the case of allivalites, and the initial compositions of inclusions can be reconstructed with high confidence. Cotectic compositions at 3.0–3.5 wt % H_2O were calculated for the average compositions of inclusions from each sample (Table 7, Fig. 10). The compositions of melt inclusions were corrected by the method of reverse fractionation to equilibrium with their host minerals (Danyushevsky et al., 2002b) at FeO_{tot} values determined by the above-described method (using the model of olivine–melt equilibrium by Ford, 1983) and an oxygen fugacity of NNO + 1. The corrected compositions of melt inclusions are given in Table 8. They fall within the range 45–55 wt % SiO_2 and 4.2–9.0 wt % MgO and reflect the wide range of olivine composition ($Fo_{69–81}$).

Table 4. Compositions of minerals and glass from the groundmass of allivalites, wt %

Sample no.	SiO_2	TiO_2	Al_2O_3	FeO_{tot}	MnO	MgO	CaO	Na_2O
Plagioclase								
Ksud-2 (5)	50.58 (0.93)	–	29.88 (0.57)	1.32 (0.25)	–	0.20 (0.04)	14.49 (0.73)	3.23 (0.38)
Kudr-E-03 (3)	53.69 (2.4)	–	27.74 (1.69)	1.44 (0.22)	–	0.24 (0.04)	12.38 (1.51)	4.09 (0.72)
115a (1)	51.95	–	28.67	1.85	–	0.27	13.76	3.17
Clinopyroxene								
Ksud-2 (4)	45.53 (1.78)	1.58 (0.16)	7.37 (1.93)	14.51 (1.63)	0.31 (0.08)	10.92 (2.2)	19.12 (3.62)	0.40 (90.12)
Kudr-E-03 (2)	48.74 (0.14)	1.32 (0.32)	2.91 (0.19)	17.74 (0.46)	0.55 (0.02)	12.86 (0.22)	15.23 (0.40)	0.27 (0.19)
115a (1)	48.11	0.99	4.98	17.22	0.47	14.78	12.91	0.12
Titanomagnetite								
Ksud-2 (2)	0.59 (0.34)	7.73 (0.95)	3.92 (1.09)	83.70 (2.19)	0.57 (0.06)	1.39 (0.28)	0.20 (0.08)	–
Kudr-E-03 (2)	0.25 (0.09)	11.51 (6.63)	3.55 (1.90)	78.87 (4.52)	0.44 (0.04)	2.97 (0.74)	0.17 (0.08)	–
Groundmass glass								
Ksud-2 (3)	71.04 (0.94)	0.63 (0.28)	14.87 (0.26)	3.96 (1.04)	0.16 (0.02)	0.47 (0.24)	3.52 (0.35)	3.16 (0.20)
Kudr-E-03 (5)	61.23 (1.2)	1.90 (0.28)	11.29 (0.26)	12.54 (1.04)	0.27 (0.02)	2.02 (0.24)	6.50 (0.35)	2.74 (0.20)
Groundmass								
Ksud-2 (8)	49.44 (0.53)	0.80 (0.12)	18.16 (2.10)	10.29 (1.96)	0.18 (0.06)	4.87 (1.42)	11.42 (1.62)	2.41 (0.31)
Kudr-E-03 (1)	55.75	1.67	15.16	11.18	0.25	2.84	8.02	3.11
115a (2)	51.10 (0.31)	0.80 (0.08)	15.45 (0.07)	12.97 (0.78)	0.25 (0.02)	7.99 (0.00)	9.43 (0.21)	1.60 (0.11)
Andesite mantle around allivalite								
Kudr-E-03 (2)	62.73 (0.06)	0.96 (0.11)	15.45 (0.11)	7.55 (0.01)	0.11 (0.04)	1.87 (0.14)	6.62 (0.10)	3.26 (0.19)

Sample no.	K_2O	Cr_2O_3	NiO	P_2O_5	S	Cl	Total	Mg# or *An* mol %
Plagioclase								
Ksud-2 (5)	0.04 (0.03)	–	–	–	–	–	99.74	71.3 (3.4)
Kudr-E-03 (3)	0.09 (0.02)	–	–	–	–	–	99.69	62.5 (6.8)
115a (1)	0.03	–	–	–	–	–	99.75	70.6
Clinopyroxene								
Ksud-2 (4)	–	–	–	–	–	–	99.74	57.0 (4.3)
Kudr-E-03 (2)	–	–	–	–	–	–	99.63	56.4 (1.1)
115a (1)	–	–	–	–	–	–	99.58	60.5
Titanomagnetite								
Ksud-2 (2)	–	0.08 (0.12)	0.51 (0.04)	–	–	–	98.69	
Kudr-E-03 (2)	–	0.16 (0.03)	0.49 (0.09)	–	–	–	98.42	
Groundmass glass								
Ksud-2 (3)	1.37 (0.08)	–	–	0.33 (0.12)	0.03 (0.04)	0.40 (0.13)	99.95	
Kudr-E-03 (5)	0.82 (0.08)	–	–	0.22 (0.12)	0.07 (0.04)	0.21 (0.13)	99.81	
Groundmass								
Ksud-2 (8)	0.25 (0.04)	–	–	0.09 (0.06)	0.13 (0.07)	0.14 (0.06)	98.18	
Kudr-E-03 (1)	0.45	–	–	0.10		0.15	98.68	
115a (2)	0.07 (0.03)	–	–	0.07 (0.01)	0.07 (0.03)	0.04 (0.00)	99.82	
Andesite mantle around allivalite								
Kudr-E-03 (2)	0.97 (0.08)	–	–	0.24 (0.04)	0.07 (0.01)	0.08 (0.02)	99.91	

Table 5. Compositions of minerals from crystallized melt inclusions, wt %

Component	Clinopyroxene								Amphibole					*Pl*
	C-305/7	C-305/7	C-305/7	C-305/7	C-305/7	C-305/7	C-305/7	C-305/7	C-305/7	C-305/7	C-305/7	115a	Ks-3	C-305/7
SiO_2	38.59	39.26	38.79	39.59	38.76	39.49	37.53	38.79	39.41	39.65	39.38	48.92	42.08	46.87
TiO_2	1.74	1.56	1.43	1.51	1.42	1.58	2.43	1.74	1.68	1.18	1.31	1.22	1.55	–
Al_2O_3	15.26	14.23	16.10	13.45	14.67	14.30	15.07	14.54	17.34	15.19	15.24	15.86	17.02	33.94
FeO_{tot}	17.00	16.94	17.78	17.49	18.01	15.37	16.64	16.67	19.04	19.03	19.10	16.75	18.80	1.10
MnO	0.14	0.33	0.14	0.25	0.43	0.12	0.14	0.32	0.29	0.25	0.23	0.56	0.24	–
MgO	5.34	6.03	6.50	6.07	5.73	6.07	5.34	5.55	7.74	8.04	7.22	3.71	7.46	0.33
CaO	21.26	21.14	17.77	20.24	19.35	22.24	21.86	21.48	11.49	14.58	15.71	12.75	11.07	17.83
Na_2O	0.03	0.11	0.83	0.38	0.80	0.19	0.22	0.13	1.97	1.16	1.19	0.25	2.19	1.46
K_2O	–	–	–	–	–	–	–	–	0.14	0.10	0.06	0.44	–	0.01
Total	99.4	99.6	99.4	99.0	99.2	99.4	99.2	99.2	99.1	99.2	99.4	100.5	100.4	101.5
Mg# or *An* mol %	35.9	38.8	39.5	38.2	36.2	41.3	36.4	37.2	42.0	42.9	40.2	28.3	73.6	87.1
Si	1.498	1.517	1.490	1.539	1.500	1.523	1.458	1.506	5.769	5.955	6.005	7.182	6.055	
Ti	0.051	0.045	0.041	0.044	0.041	0.046	0.071	0.051	0.185	0.133	0.150	0.135	0.168	
Al^{IV}	0.502	0.483	0.510	0.461	0.500	0.477	0.542	0.494	2.231	2.045	1.995	0.818	1.945	
Al^{VI}	0.197	0.165	0.218	0.155	0.169	0.172	0.148	0.172	0.761	0.644	0.744	1.926	0.940	
Fe^{3+}	0.206	0.235	0.271	0.246	0.308	0.227	0.268	0.230	0.914	0.087	0.000	0.000	0.645	
Fe^{2+}	0.346	0.313	0.300	0.323	0.275	0.268	0.273	0.311	1.417	2.304	2.436	2.056	1.617	
Mn	0.005	0.011	0.005	0.008	0.014	0.004	0.005	0.011	0.035	0.032	0.030	0.070	0.029	
Mg	0.309	0.348	0.372	0.352	0.330	0.349	0.309	0.321	1.688	1.801	1.640	0.813	1.601	
Ca	0.884	0.875	0.731	0.843	0.802	0.919	0.910	0.894	1.801	2.346	2.566	2.005	1.706	
Na	0.002	0.008	0.062	0.029	0.060	0.014	0.016	0.010	0.558	0.337	0.352	0.072	0.611	
K	0.002	–	0.003	0.001	–	–	–	–	0.026	0.020	0.012	0.082	–	
O	6	6	6	6	6	6	6	6	23	23	23	23	23	
Cations	4	4	4	4	4	4	4	4	13	13	13	13	13	
Ts, %	50.2	48.3	51.0	46.1	50.0	47.7	54.2	49.4						

Note: *Pl* is plagioclase, and *Ts*, % is the fraction of the Tschermak component in clinopyroxene composition.

The calculated melt compositions correspond in general to the fields of the groundmass of allivalites (Fig. 9). The contents of MgO, CaO, and Al_2O_3 are positively correlated with the forsterite mole fraction of the host olivine, whereas SiO_2 shows the opposite trend. This is in good agreement with the suggested simultaneous crystallization of olivine and plagioclase.

Temperatures of Allivalite Formation

Crystallization temperatures were estimated from the equilibrium between melts in the inclusion and host olivines using the olivine–melt model of Danyushevsky (2001) at an oxygen fugacity of NNO + 1 and 3.0–3.5 wt % H_2O. The calculated temperatures range from 970 to 1080°C (Table 8) and are significantly lower than the temperatures experimentally obtained by Selyangin (1975) for melt inclusions in minerals from the allivalites of Malyi Semyachik Volcano (1430–1180°C). We managed to attain the complete homogenization of a melt inclusion in olivine from allivalite sample 115a (Golovnin Volcano) in a thermometric experiment with a visual control at a temperature of 1243 ± 10°C (sample was kept at T > 1000°C for 6 min). The higher (compared with the calculated values) experimental temperatures could be related to a significant loss of water from the inclusion during the experiments. However, the appearance of magnetite, which usually accompanies water loss during experiments, was never observed. Thermometric experiments were carried out under visual inspection with 16 inclusions in olivine from sample C-305/7 (Zavaritskii Volcano). Complete homogenization was observed in seven experiments at temperatures of 1107–1132°C. Frolova et al. (2000) reported homogenization temperatures of 1050–1100°C for some melt inclusions in

Table 6. Compositions of melt inclusions in olivine, wt %

Sample no.	Inclusion no.	SiO_2	TiO_2	Al_2O_3	FeO_{tot}	MnO	MgO	CaO	Na_2O	K_2O	P_2O_5	H_2O	*Fo*, mol %	Inclusion size, μm
Si-5	Ci11-G1	50.50	0.90	18.79	11.27	0.15	3.81	12.24	2.02	0.14	0.17		78.7	60
Ks-1	G17-1	48.94	0.72	14.06	15.64	0.50	8.45	9.57	1.89	0.16	0.06		75.2	60
Ks-1	18-1G	50.28	0.85	15.55	14.61	0.47	4.69	11.06	2.17	0.21	0.11		75.8	59
Ks-1	G20-1	49.45	0.63	13.85	14.65	0.44	10.13	9.07	1.38	0.32	0.09		75.6	105
Ks-1	G21-1	49.79	0.72	14.84	14.77	0.44	7.27	10.16	1.59	0.24	0.19		75.6	57
Ks-1	G22-1	49.63	0.80	14.16	15.65	0.27	7.98	9.77	1.44	0.27	0.04		75.7	60
Ks-1	G22-2	49.64	0.77	15.17	15.37	0.23	6.90	10.13	1.43	0.28	0.08		75.9	50
Ks-1	G-32-1	51.94	0.90	15.77	14.02	0.46	3.82	10.83	2.00	0.21	0.06		75.3	42
Ks-1	G32-2	53.01	1.09	17.44	12.03	0.27	1.80	11.78	2.27	0.22	0.08		74.9	21
Ks-1	G33-1	50.36	0.75	15.21	14.46	0.41	6.66	10.15	1.66	0.25	0.10		76.0	40
Ks-1	G33-2	49.50	0.72	14.84	14.93	0.33	7.73	9.80	1.69	0.33	0.14		75.7	75
Ks-1	G34-1	50.73	0.81	14.98	14.70	0.38	5.41	10.78	1.91	0.20	0.10	3.00	75.2	60
Ks-1	G34-2	51.08	0.92	16.08	14.23	0.36	3.36	11.24	2.53	0.12	0.10		75.5	30
Ks-1	G35-1	51.15	0.82	14.97	14.76	0.38	5.24	10.45	1.96	0.21	0.06	3.11	75.4	55
Ks-1	G36-1	49.04	0.70	13.75	15.17	0.41	9.72	9.26	1.17	0.56	0.23		75.4	80
Ks-1	G37-1	51.04	0.73	15.24	14.75	0.38	4.63	10.98	2.00	0.22	0.04	3.00	75.4	55
Ks-1	G38-1	49.67	0.82	14.88	14.52	0.45	7.83	9.72	1.51	0.44	0.16		75.2	55
Ks-1	G38-2	50.23	0.66	15.35	13.81	0.24	7.32	9.79	1.94	0.56	0.10		75.7	55
Ks-1	G-39-1	50.34	0.67	13.97	13.95	0.28	9.76	8.74	1.80	0.37	0.12		74.9	110
Ks-3	G-40-1	49.50	0.75	16.30	12.54	0.10	7.35	11.30	1.85	0.24	0.07		80.2	65
Ks-3	G-42-1	49.99	0.89	18.60	11.00	0.28	4.08	12.27	2.41	0.37	0.11		79.7	40
Ks-3	G29-1	49.38	0.94	18.18	11.55	0.16	4.63	12.17	2.55	0.29	0.16		80.7	40
Ks-3	G30-3	50.19	1.01	16.79	11.61	0.17	6.66	11.09	2.08	0.24	0.16		80.1	60
Ks-3	G44-1	48.93	0.59	17.83	10.64	0.36	8.57	11.12	1.65	0.19	0.12		80.6	60
Ks-3	G47-1	49.59	0.96	16.74	11.71	0.25	7.31	11.21	1.78	0.24	0.21	2.92	80.2	60
Ks-3	G51-1	49.07	0.68	15.94	12.05	0.32	8.78	10.65	1.96	0.24	0.30		80.6	60
C-305/7	M1	47.05	0.79	16.82	17.48	0.24	4.48	11.38	1.40	0.13	0.23		79.0	
C-305/7	M2	48.33	0.87	19.35	14.07	0.24	1.99	13.10	1.76	0.16	0.13		79.0	
C-305/7	M3	46.68	0.73	18.09	15.36	0.19	3.95	12.59	2.05	0.14	0.22		78.9	
C-305/7	M4	48.09	0.76	17.54	14.96	0.15	4.17	12.05	1.97	0.12	0.19		79.4	
C-305/7	M5	48.04	0.93	16.93	14.91	0.42	5.24	11.71	1.54	0.14	0.16	3.40	79.2	
C-305/7	M6	49.59	0.86	20.68	11.44	0.19	3.79	11.48	1.65	0.19	0.13		82.3	
C-305/7	M9	46.41	0.49	19.32	12.25	0.25	9.57	10.27	1.05	0.24	0.14		79.0	
C-305/7	M10	48.41	0.83	15.74	14.80	0.05	7.10	10.80	1.93	0.10	0.24	3.02	78.8	
C-305/7	M12	48.90	0.83	16.92	13.71	0.10	5.70	11.56	1.92	0.18	0.16	3.20	79.0	
C-305/7	M13	48.43	0.96	17.72	14.59	0.18	4.02	11.83	1.92	0.15	0.20		78.8	
C-305/7	M16	46.86	0.69	18.73	14.60	0.18	11.02	6.60	0.83	0.27	0.23		78.5	
Kudr-E-03	KudrG67-1	50.82	0.94	20.10	10.77	0.35	2.37	11.98	2.22	0.26	0.20		77.0	30
Kudr-E-03	KudrG69-1	50.50	0.77	18.37	11.95	0.22	3.55	11.95	2.10	0.36	0.23		78.0	35
Kudr-E-03	KudrG71-1	49.98	0.76	17.43	13.10	0.30	5.15	11.21	1.73	0.17	0.17	3.28	78.5	90
Kudr-E-03	KudrG71-2	51.81	0.93	20.20	9.73	0.24	2.02	12.25	2.44	0.27	0.10	2.85	79.0	20
Kudr-E-03	KudrG71-3	51.05	0.89	18.48	11.64	0.27	3.26	11.73	2.31	0.24	0.15		78.5	40
Kudr-E-03	KudrG72-1	50.24	0.85	18.37	12.15	0.10	3.79	11.75	2.45	0.20	0.11		78.5	55
Kudr-E-03	KudrG72-2	50.87	0.82	17.83	10.57	0.47	5.88	10.69	2.20	0.47	0.21		78.3	30

Table 6. (Contd.)

Sample no.	Inclusion no.	SiO_2	TiO_2	Al_2O_3	FeO_{tot}	MnO	MgO	CaO	Na_2O	K_2O	P_2O_5	H_2O	*Fo*, mol %	Inclusion size, μm
115a	115a-G58	48.90	0.72	17.56	14.09	0.35	5.28	11.03	1.92	0.12	0.03		76.3	60
115a	115a-G59	49.43	0.82	19.26	12.60	0.17	3.15	12.29	1.97	0.11	0.22		76.5	45
115a	115a-G60	50.17	0.73	18.95	12.88	0.19	2.81	12.36	1.66	0.11	0.13		75.9	55
115a	115a-G55	50.04	0.85	19.75	11.81	0.35	2.51	12.77	1.74	0.08	0.10		76.0	40
115a	115a-G57	49.34	0.84	18.68	13.69	0.20	3.24	11.93	1.84	0.07	0.18		76.0	90
6636/gp-15	G104-1	57.67	0.87	17.14	10.20	0.31	1.73	8.53	3.18	0.16	0.21		71.1	45
6636/gp-15	G105-1	56.83	0.92	17.24	11.44	0.16	1.63	8.57	2.86	0.15	0.21		70.0	30
6636/gp-15	G105-2	55.40	0.82	16.44	12.72	0.37	2.84	8.42	2.64	0.23	0.13		69.8	40
6636/gp-15	G106-1	53.64	1.01	16.28	14.10	0.36	3.58	7.87	2.74	0.09	0.31		69.9	80
6636/gp-15	G111-1	56.47	0.91	17.09	12.06	0.34	2.04	8.07	2.67	0.21	0.13		70.2	50
6636/gp-18	G-114-1	49.48	0.76	16.65	13.93	0.06	5.95	11.63	1.31	0.10	0.13		78.0	100
6636/gp-18	G117-2	50.11	0.79	18.70	12.94	0.33	2.83	12.29	1.64	0.11	0.25		77.7	30
6636/gp-18	G-118-1	48.88	0.60	16.52	14.12	0.15	8.19	10.17	1.09	0.14	0.15	1.11	78.4	70

Note: The analyses were recalculated to anhydrous totals of 100%. *Fo* is the Mg# value of host olivine.

minerals from the same sample. The lowest homogenization temperatures for sample C-305/7 indicate good preservation of inclusions in this sample with respect to fluid components, which is supported by the high measured H_2O contents (3.0–3.4 wt %) in the glasses of these inclusions (Table 6).

DISCUSSION

Allivalite analyses were reported by many authors (Bogoyavlenskaya and Erlikh, 1969; Volynets et al., 1978; Dril', 1988; Sheimovich, 1966; Selyangin, 1974; Frolova et al., 2000). As can be seen in Fig. 10, the bulk compositions of allivalites show considerable variations in the contents of essential components of olivine and plagioclase, the main rock-forming minerals (Al_2O_3, MgO, FeO, and CaO). Such variations are attributed to substantial variations in olivine and plagioclase proportions in allivalite samples.

Many researchers (e.g., Frolova et al., 2000) pointed out stable compositions of olivine and plagioclase in all allivalites and distinguished the persistent assemblage $Fo_{78–81}$–$An_{92–96}$. The investigation of a more representative collection showed that the stability of mineral compositions holds only for individual samples. For instance, we studied several samples of allivalites from Ksudach Volcano and observed variations in olivine composition in any particular sample within 1–2% of the forsterite component. However, the composition of olivine varied among the samples from Fo_{81} to Fo_{75}. The composition of plagioclase ranged from An_{96} to An_{89}. In general, there is a positive correlation between the forsterite mole fraction of olivine and anorthite mole fraction of plagioclase from allivalites (Fig. 3).

Evidence for the Magmatic Origin of Allivalites

The presence of numerous primary melt inclusions in olivine, plagioclase, and clinopyroxene (Frolova et al., 2000; this study) unequivocally demonstrates that the mineral of allivalites crystallized from a melt. In addition to melt inclusions, the olivines contain solid inclusions of plagioclase, clinopyroxene, chrome spinel, and titanomagnetite; and the plagioclases contain olivine inclusions. The presence of olivine inclusions in plagioclase and plagioclase inclusions in olivine indicates their simultaneous crystallization.

The magmatic origin of the minerals of allivalites is also suggested by the high contents of CaO in olivine (0.1–0.3 wt %) and FeO* in plagioclase (0.5–1.85 wt %) (Tables 2, 3). Olivine from mantle peridotites and metamorphic rocks contains less than 0.1 wt % CaO, as compared with more than 0.15 wt % CaO in most magmatic olivines (Simkin and Smith, 1970). The high contents of CaO in olivine from allivalites (0.17–0.21 wt %) indicate its crystallization from a melt. Similarly, the incorporation of Fe^{3+} in the structure of plagioclase is an indicator for its magmatic origin. Figure 6 shows the fields of plagioclase compositions from volcanic, intrusive, and metamorphic rocks. The compositions of plagioclase from allivalites fall within the field of magmatic plagioclases.

Revision of Hypotheses for the Origin of Allivalites

In general, allivalite are contrastingly different in composition from their host rocks. They are significantly enriched in Al_2O_3, CaO, and MgO but depleted in SiO_2 compared with island-arc volcanics (Fig. 10). It can be supposed that such compositional differences

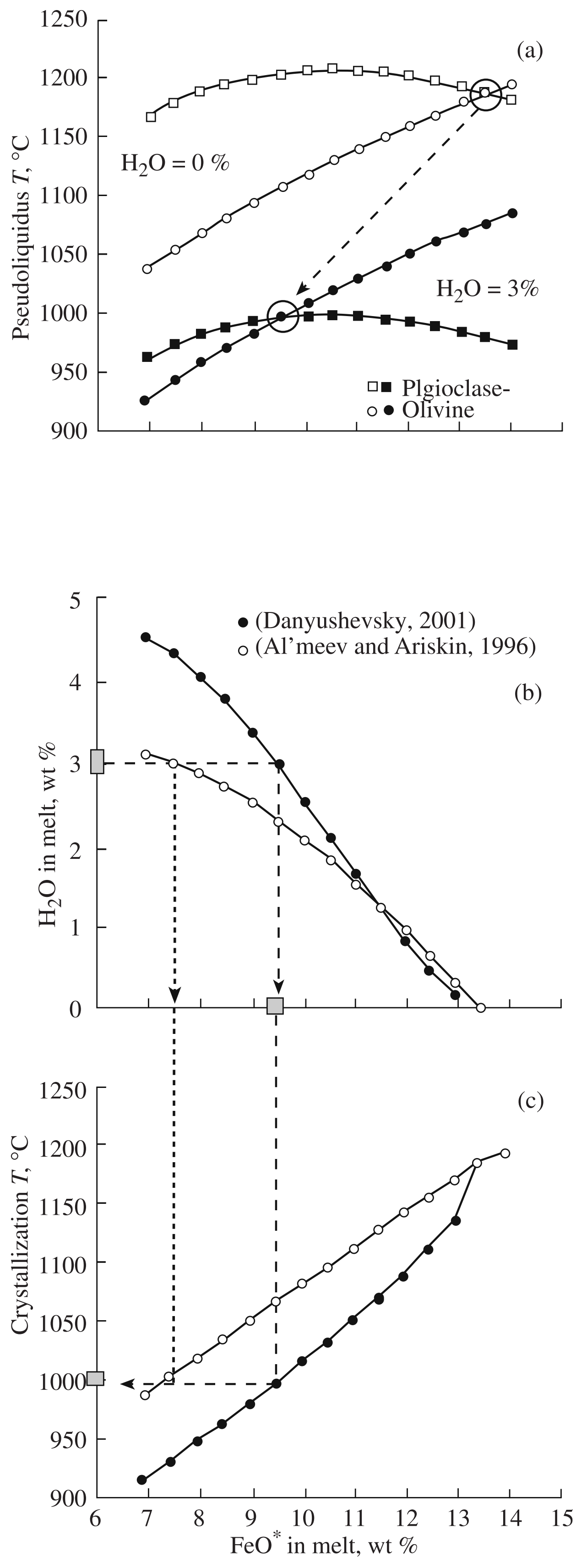

are related to either the existence of a specific melt or the processes of crystal fractionation with separation and accumulation of olivine and plagioclase.

Some authors (e.g., Syvorotkin, 1996) supposed the existence of a specific allivalite melt of ultramafic composition, which separated from a basaltic magma owing to liquid immiscibility. Assuming such a mechanism, it is difficult to explain the banded structures of some allivalites, in which the boundaries of enclaves distinctly cut the banding. In this study, we showed that melt inclusions in the minerals of allivalites correspond to the compositions of basalts and are strongly different from the bulk compositions of allivalites. Thus, the supposition of the existence of a specific melt producing allivalites is discredited. The initial melts of allivalites, the compositions of which were estimated from the analyses of melt inclusions in olivine, form a common trend with volcanic rock series (Fig. 10) and belong to the same low-potassium island-arc tholeiite series. They correspond to the most magnesian (least fractionated) rock varieties with respect to all components (except for Al_2O_3 and MgO). Such relationships between the compositions of melts and volcanics indicate that the olivine–plagioclase cumulates were formed only during the earliest stages of melt fractionation in a magma chamber.

Amma-Miyasaka and Nakagawa (2002) studied allivalites from Miyakejima Volcano (Izu–Bonin island

Fig. 8. Illustration of the method for the determination of the initial composition of cotectic melt trapped in inclusions in olivine by the example of the average composition of melt inclusions from sample Ks-1. (a) Calculated pseudoliquidus temperatures of olivine (Ford et al., 1983) and plagioclase (Ariskin et al., 1993) crystallization for the compositions of melt in inclusions recalculated to various initial FeO* (Danyushevsky et al., 2000) and water contents in the melt (1 and 3 wt %). The liquidus temperatures were corrected for the influence of water using the model of Danyushevsky (2001). The cotectic compositions corresponding to the identical psedoliquidus temperatures of the minerals are shown by circles. The dashed arrow indicates the shift of cotectic compositions toward lower FeO* contents owing to an increase in the melt water content. (b) Cotectic contents of H_2O and FeO* calculated using two models (Danyushevsky, 2001; Al'meev and Ariskin, 1996). The measured H_2O content in the melt (3 wt %) allows us to estimate the initial content of FeO* as 9.5 wt % using the model of Danyushevsky (2001) and, subsequently, the contents of other components. The model of Al'meev and Ariskin (1996) yielded a lower initial FeO* content of 7.5 wt %, which does not correspond to the compositions of typical low-potassium basalts from Kamchatka and the Kuril Islands (9–11 wt % FeO). The initial FeO* content calculated by the model of Danyushevsky (2001) is in good agreement with the rock compositions, and it was, therefore, used in our study. (c) Dependence of the temperatures of cotectic crystallization on the content of FeO* at variable H_2O content in the melt. The diagrams illustrate how the contents of H_2O and FeO* in the cotectic melt can be used to estimate the equilibrium temperature. The temperature estimates based on various models (Danyushevsky, 2001; Al'meev and Ariskin, 1996) are identical in this case.

Table 7. Cotectic compositions of melts in allivalites, wt %

Component	Ksudach		Il'inskii	Zavaritskii	Kudryavyi	Golovnin		
	Ks-1	Ks-3	Si-5	C-305/7	Kudr-E-03	115a	6636/gp-15	6636/gp-18
				Average compositions of melt inclusions				
SiO_2	50.69	49.54	49.47	46.27	50.24	48.08	54.97	49.41
TiO_2	0.81	0.80	0.88	0.82	0.84	0.77	0.87	0.72
Al_2O_3	15.33	16.34	18.41	18.87	18.49	18.27	17.15	17.26
FeO_{tot}	14.38	11.25	11.04	14.53	11.30	12.62	12.23	13.64
MnO	0.37	0.26	0.15	0.24	0.28	0.24	0.33	0.18
MgO	6.16	6.68	3.73	6.05	3.68	3.29	2.07	5.65
CaO	10.38	12.32	11.99	10.18	11.53	11.71	8.63	11.34
Na_2O	1.86	1.99	1.98	1.46	2.19	1.77	2.89	1.34
K_2O	0.28	0.28	0.14	0.21	0.28	0.10	0.17	0.12
P_2O_5	0.11	0.21	0.17	0.22	0.17	0.13	0.19	0.18
Cr_2O_3	0.05	0.67	2.07	0.68	1.27	2.99	0.91	0.40
Total	100.41	100.33	100.03	99.53	100.25	99.98	100.41	100.24
Fo, mol %	75.5	80.3	78.7	79.3	78.2	76.1	70.2	78.1
An, mol %	92.9	93.7	89.6	94.4	94.1	96.2	94.4	96.2
				Cotectic compositions for 3.0–3.5 wt % H_2O				
SiO_2	52.47	50.42	50.17	47.18	50.21	49.22	54.98	50.47
TiO_2	0.90	0.84	0.86	0.84	0.81	0.76	0.85	0.76
Al_2O_3	17.09	17.26	18.08	19.31	17.74	17.98	16.77	18.2
FeO_{tot}	9.97	9.53	10.52	12.50	11.04	12.05	11.03	10.54
MnO	0.41	0.27	0.15	0.25	0.27	0.24	0.32	0.19
MgO	4.86	5.84	5.97	7.30	6.09	6.00	4.19	5.92
CaO	11.57	13.01	11.78	10.41	11.07	11.52	8.44	11.96
Na_2O	2.07	2.10	1.94	1.49	2.10	1.74	2.83	1.41
K_2O	0.31	0.30	0.14	0.21	0.27	0.10	0.17	0.13
P_2O_5	0.12	0.22	0.17	0.23	0.16	0.13	0.19	0.19
***T* (H_2O) Dan**	**970**	**999**	**1003**	**1048**	**1018**	**1005**	**982**	**996**
H_2O calc (Dan)	**3.2**	**3.0**	**3.3**	**3.0**	**3.0**	**3.2**	**3.2**	**3.21**
Fe_2O_3	2.22	2.12	2.34	2.78	2.45	2.68	2.45	2.34
FeO	7.97	7.62	8.41	10.00	8.83	9.64	8.82	8.43

Note: *Fo* and *An* are the average Mg# of olivine and anorthite mole fraction of plagioclase for the particular sample; $T(H_2O)$ Dan is the temperature of cotectic crystallization of olivine and plagioclase from the initial melt of allivalite calculated using the model of Danyushevsky (2001); H_2O calc (Dan) is the content of water in the cotectic melt; Fe_2O_3 and FeO are the calculated contents of ferric and ferrous iron oxides in melt at an oxygen fugacity corresponding to NNO + 1.

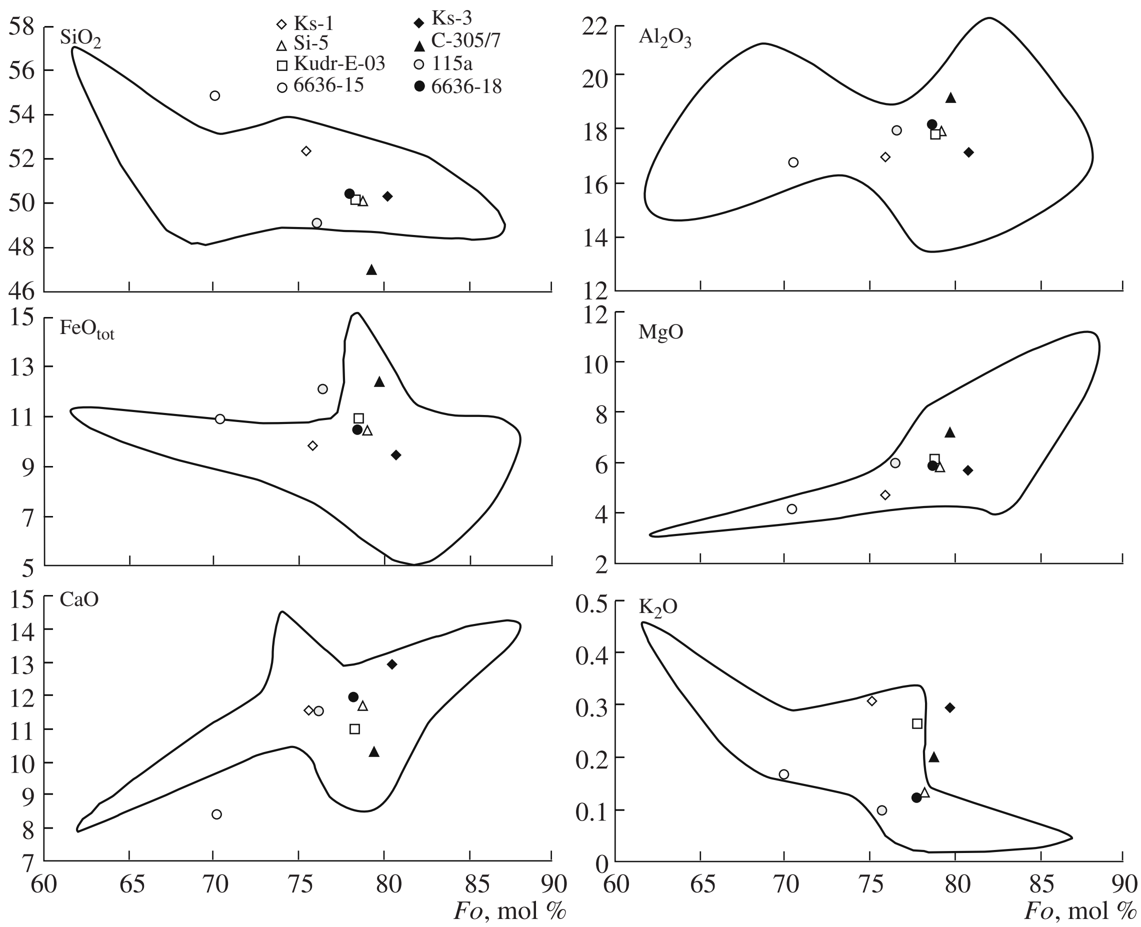

Fig. 9. Contents of chemical elements (wt %) in melt inclusions as functions of the forsterite mole fraction of the host olivine. The sampling sites are given in Table 1. Also shown is the field of the compositions of interstitial materials from allivalites. The composition of olivine in equilibrium with the composition of the interstitial material was calculated using the Petrolog program.

arc) and named them M-type crystal clots, i.e., megacryst intergrowths. They noted traces of solid-state deformation and recrystallization in them, including kink-band structures in olivine, spherical shapes of olivine inclusions in plagioclase, and obliteration of zoning in plagioclases. These authors argued that such processes require considerable time and could occur in the cumulate layer of a magma chamber. In our opinion, the obliteration of plagioclase zoning is hardly possible because of the very low CaAl–NaSi diffusion coefficients in plagioclase (Grove and Baker, 1984). Moreover, in the allivalite samples studied by us, the compositions of solid inclusions of olivine in plagioclase and plagioclase in olivine coincide with the compositions of large grains. This suggests that the compositions of minerals were not significantly affected by recrystallization. Amma-Miyasaka and Nakagawa (2002) supposed that the allivalites are fragments of an individual troctolitic intrusion. In such a case, the compositions of melts in melt inclusions should have been more variable and significantly different from the compositions of volcanic rocks. In addition, the coexistence of iron-rich olivine and calcium-rich plagioclase are not characteristic of troctolite intrusions in general (e.g., Lungaard et al., 2002).

Masurenkov (1974) evaluated the possibility of formation of olivine–anorthite nodules via the recrystallization of xenoliths of amphibole-bearing country rocks owing to the reaction of amphibole decomposition and concurrent removal of sodium. This mechanism of allivalite formation is in conflict with the abundance of primary melt inclusions in allivalite minerals, small variations in the compositions of trapped melts, and their similarity to the compositions of volcanic series. The replacement of xenoliths by an olivine–anorthite aggregate would inevitably have resulted in the preservation of relics of primary minerals and traces of reaction replacement, including zoning and chemical variations in minerals. In such a case, the occurrence of host rock xenoliths with rims of olivine–anorthite aggregates should be expected.

Volynets et al. (1978) examined the suggestion of the mantle origin of allivalites as residues after the derivation of basaltic melts. The melting of mantle lherzolites under island-arc mantle conditions must leave

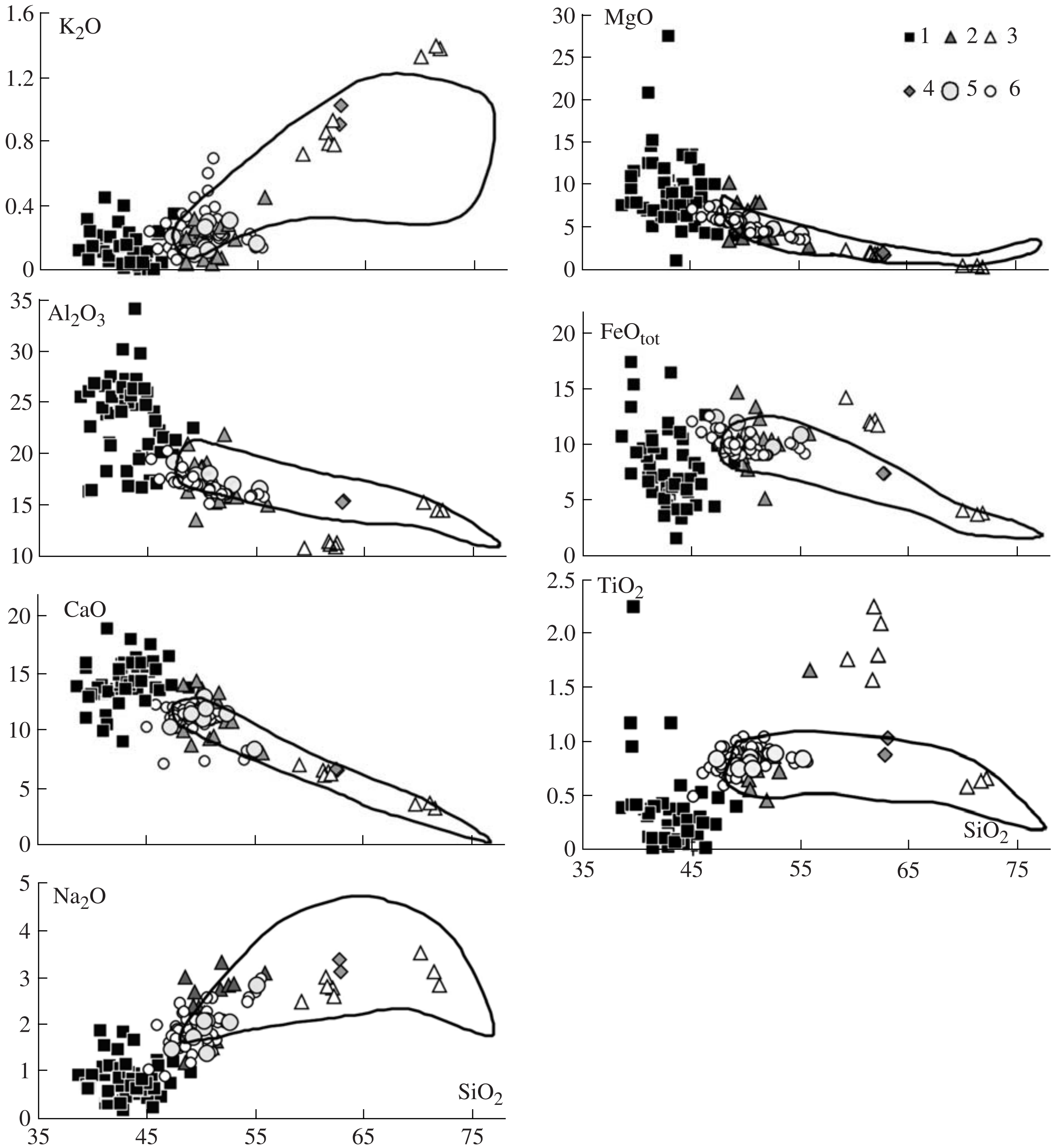

Fig. 10. Petrochemical diagrams. (*1*) Allivalites after Bogoyavlenskaya and Erlikh (1969), Volynets et al. (1978), Dril' (1988), Selyangin (1974), Frolova et al. (2000), and Sheimovich (1966); (*2*) crystallized groundmass material; (*3*) groundmass glass; (*4*) fine-grained rim zone of allivalite (Kudryavyi Volcano); (*5*) cotectic composition of melt inclusions (average for a particular sample); and (*6*) composition of melt inclusions recalculated to cotectic equilibria. The field of volcanic rocks from Kamchatka and the Kuril Islands is based on the data of *Active Volcanoes…* (1991); Dril' (1988); Popolitov and Volynets (1981); Frolova et al. (2000); Bailey et al. (1987); Gorshkov (1970); Ostapenko et al. (1967); and Zharinov (1988). Oxide contents are in wt %.

dunite–harzburgite residues, whereas the plagioclase component must escape into the basaltic melt. The island-arc mantle is characterized by high degrees of melting (>20%), which corresponds to olivine compositions with forsterite mole fractions of at least Fo_{90}, whereas olivine $Fo_{75–81}$ occurs in allivalites. Chrome spinel is widespread in mantle rocks, whereas titanomagnetite is typical of allivalites.

The model of early glomerophyric intergrowths considered by Frolova et al. (1989) is not appropriate for allivalite origin, because such intergrowths should be immersed in a magma in equilibrium with them,

Table 8. Compositions of melt inclusions recalculated to account for iron-loss effect using the Petrolog program for the average cotectic melts, wt %

Sample no.	Inclusion no.	SiO_2	TiO_2	Al_2O_3	Fe_2O_3	FeO	MnO	MgO	CaO	Na_2O	K_2O	P_2O_5	H_2O	T, °C	$\log f_{O_2}$	dNNO	*Fo*	*An*	*Ol*, %	*Pl*, %
Si-5	Ci11-G1	48.66	0.85	17.49	1.48	8.58	0.14	5.78	11.43	1.89	0.14	0.16	3.40	1004.4	−9.16	−0.6	78.1	87.3	31	69
Ks-1	G17-1	50.31	0.86	16.54	1.59	8.27	0.60	4.67	11.31	2.25	0.20	0.07	3.34	972.7	−9.65	−0.7	74.4	81.0	21	79
Ks-1	18-1G	50.42	0.90	16.25	1.64	8.24	0.50	4.77	11.61	2.29	0.23	0.12	3.04	979.7	−9.54	−0.6	75.0	79.7	25	75
Ks-1	G20-1	51.08	0.76	16.67	1.43	8.45	0.54	4.87	10.95	1.68	0.39	0.11	3.07	982.0	−9.51	−0.6	74.4	87.8	26	74
Ks-1	G21-1	50.64	0.81	16.56	1.47	8.41	0.50	4.85	11.39	1.79	0.27	0.22	3.08	979.0	−9.55	−0.6	74.6	86.1	25	75
Ks-1	G22-1	51.33	0.95	16.65	1.35	8.03	0.32	4.64	11.54	1.70	0.32	0.05	3.12	970.2	−9.69	−0.6	74.6	87.4	24	76
Ks-1	G22-2	50.56	0.87	16.94	1.43	8.44	0.26	4.92	11.36	1.61	0.31	0.09	3.20	979.6	−9.54	−0.6	74.8	89.3	24	76
Ks-1	G-32-1	51.99	0.93	16.21	1.41	7.98	0.48	4.51	11.18	2.07	0.22	0.06	2.97	972.4	−9.66	−0.6	74.2	81.8	26	74
Ks-1	G32-2	51.53	1.05	16.47	1.47	7.95	0.25	4.40	11.18	2.16	0.21	0.08	3.26	965.7	−9.77	−0.7	73.9	81.7	21	79
Ks-1	G33-1	50.99	0.82	16.60	1.45	8.38	0.45	4.93	11.12	1.82	0.27	0.11	3.05	984.7	−9.46	−0.6	75.0	85.8	26	74
Ks-1	G33-2	50.29	0.81	16.60	1.67	8.73	0.37	5.08	10.99	1.90	0.37	0.16	3.01	992.9	−9.33	−0.6	74.9	84.9	26	74
Ks-1	G34-1	51.46	0.89	16.24	1.41	7.93	0.42	4.45	11.75	2.08	0.22	0.11	3.04	965.1	−9.78	−0.6	74.1	81.8	25	75
Ks-1	G34-2	50.88	0.95	16.37	1.53	7.83	0.37	4.45	11.50	2.60	0.13	0.11	3.29	968.0	−9.73	−0.7	74.8	76.8	20	80
Ks-1	G35-1	51.90	0.89	16.16	1.42	7.97	0.41	4.54	11.33	2.13	0.23	0.07	2.94	973.5	−9.64	−0.6	74.4	81.0	26	74
Ks-1	G36-1	50.93	0.87	16.80	1.34	8.00	0.51	4.58	11.36	1.44	0.70	0.28	3.20	965.4	−9.77	−0.7	74.3	91.3	23	77
Ks-1	G37-1	51.57	0.78	16.20	1.40	7.97	0.41	4.51	11.73	2.14	0.23	0.04	2.99	969.6	−9.70	−0.6	74.3	81.0	26	74
Ks-1	G38-1	50.48	0.94	16.78	1.52	8.33	0.52	4.74	11.00	1.71	0.50	0.19	3.30	973.9	−9.64	−0.7	74.3	87.8	22	78
Ks-1	G38-2	50.49	0.73	16.60	1.74	8.66	0.26	5.01	10.62	2.11	0.61	0.11	3.06	998.0	−9.26	−0.6	75.0	82.6	25	75
Ks-1	G-39-1	51.70	0.80	16.47	1.56	8.32	0.33	4.63	10.33	2.14	0.44	0.15	3.13	984.8	−9.46	−0.6	73.9	82.0	24	76
Ks-3	G-40-1	49.39	0.80	17.24	1.31	7.96	0.11	5.86	11.98	1.97	0.26	0.08	3.04	1014.6	−9.00	−0.5	79.8	85.6	48	52
Ks-3	G-42-1	48.22	0.84	17.38	1.61	8.34	0.26	5.81	11.51	2.27	0.35	0.11	3.31	1014.4	−9.01	−0.6	79.1	83.0	23	77
Ks-3	G29-1	48.05	0.91	17.46	1.55	8.03	0.16	5.94	11.73	2.47	0.28	0.16	3.28	1020.3	−8.92	−0.5	80.3	81.1	32	68
Ks-3	G30-3	49.57	1.05	17.13	1.43	7.95	0.18	5.72	11.35	2.14	0.25	0.17	3.07	1015.0	−9.00	−0.5	79.4	83.6	24	76
Ks-3	G44-1	47.86	0.60	18.02	1.45	8.90	0.36	6.56	11.26	1.69	0.20	0.12	2.98	1036.4	−8.68	−0.5	79.8	90.9	28	72
Ks-3	G47-1	49.05	1.01	17.31	1.37	8.03	0.26	5.80	11.64	1.86	0.25	0.23	3.18	1009.2	−9.08	−0.6	79.4	87.2	24	76
Ks-3	G51-1	49.00	0.75	17.21	1.37	8.03	0.35	5.93	11.54	2.14	0.26	0.33	3.09	1017.6	−8.96	−0.5	79.8	83.9	25	75
C-305/7	M1	47.45	0.84	17.60	1.65	9.22	0.25	6.25	11.94	1.48	0.14	0.25	2.93	1020.5	−8.91	−0.5	78.2	92.5	28	72
C-305/7	M2	46.94	0.81	17.77	1.70	9.20	0.22	6.19	12.08	1.63	0.15	0.13	3.18	1017.8	−8.95	−0.5	78.3	91.1	26	74
C-305/7	M3	45.93	0.72	17.61	1.99	9.46	0.19	6.31	12.30	2.02	0.14	0.22	3.13	1025.2	−8.84	−0.5	78.5	86.2	26	74
C-305/7	M4	47.59	0.76	17.49	1.62	8.78	0.16	6.00	12.06	1.98	0.13	0.20	3.23	1014.9	−9.00	−0.6	78.7	86.3	24	76

Table 8. (Contd.)

Sample no.	Inclusion no.	SiO_2	TiO_2	Al_2O_3	Fe_2O_3	FeO	MnO	MgO	CaO	Na_2O	K_2O	P_2O_5	H_2O	*T*, °C	$\log f_{O_2}$	dNNO	*Fo*	*An*	*Ol*, %	*Pl*, %
C-305/7	M5	47.90	0.96	17.44	1.51	8.64	0.43	6.01	12.10	1.60	0.14	0.16	3.10	1010.0	–9.07	–0.5	78.7	90.6	44	56
C-305/7	M6	47.90	0.81	18.88	1.29	8.64	0.18	7.06	10.48	1.53	0.18	0.12	2.94	1054.3	–8.42	–0.4	81.5	94.8	27	73
C-305/7	M9	45.09	0.50	19.55	1.77	10.57	0.25	7.12	10.39	1.07	0.24	0.15	3.30	1045.6	–8.55	–0.5	78.2	97.3	27	73
C-305/7	M10	48.80	0.91	17.21	1.49	8.26	0.06	5.65	11.85	2.12	0.11	0.27	3.27	1005.2	–9.14	–0.6	78.5	84.1	48	52
C-305/7	M12	48.49	0.86	17.32	1.53	8.49	0.11	5.77	11.88	1.97	0.19	0.17	3.22	1008.8	–9.09	–0.6	78.4	85.9	33	67
C-305/7	M13	47.74	0.96	17.49	1.66	8.77	0.19	5.87	11.72	1.91	0.15	0.21	3.34	1008.6	–9.09	–0.6	78.2	87.2	23	77
C-305/7	M16	46.59	0.77	20.44	1.75	11.11	0.20	7.52	7.15	0.92	0.29	0.26	3.00	1073.1	–8.16	–0.4	77.5	97.3	28	72
Kudr-E-03	KudrG67-1	48.02	0.82	17.35	2.01	9.71	0.30	6.09	10.36	1.94	0.22	0.18	3.00	1024.9	–8.85	–0.5	76.6	86.5	36	64
Kudr-E-03	KudrG69-1	48.82	0.73	17.10	1.69	8.91	0.21	5.82	11.16	1.97	0.34	0.22	3.05	1013.4	–9.02	–0.5	77.4	85.4	34	66
Kudr-E-03	KudrG71-1	49.17	0.76	17.21	1.54	8.94	0.30	5.98	11.10	1.73	0.17	0.17	2.93	1016.0	–8.98	–0.5	77.6	88.4	28	72
Kudr-E-03	KudrG71-2	48.91	0.81	17.41	1.65	8.85	0.21	6.06	10.59	2.13	0.24	0.09	3.05	1025.9	–8.83	–0.5	78.4	84.5	28	72
Kudr-E-03	KudrG71-3	49.30	0.83	17.07	1.68	8.77	0.25	5.80	10.87	2.15	0.23	0.14	2.92	1022.0	–8.89	–0.5	77.8	83.4	27	73
Kudr-E-03	KudrG72-1	48.64	0.80	17.19	1.77	8.89	0.10	5.96	11.03	2.30	0.19	0.11	3.02	1022.7	–8.88	–0.5	78.1	82.0	35	65
Kudr-E-03	KudrG72-2	49.29	0.80	17.14	1.71	8.73	0.45	5.76	10.30	2.14	0.45	0.21	3.01	1022.7	–8.88	–0.5	77.7	83.8	26	74
115a	115a-G58	47.93	0.71	17.32	1.98	9.74	0.35	5.89	10.92	1.91	0.12	0.03	3.10	1016.6	–8.97	–0.5	76.0	86.7	39	61
115a	115a-G59	47.41	0.74	17.46	1.99	9.83	0.15	6.00	11.17	1.80	0.10	0.20	3.13	1016.7	–8.97	–0.5	76.2	88.3	46	54
115a	115a-G60	48.39	0.68	17.49	1.70	9.48	0.17	5.59	11.43	1.54	0.11	0.12	3.30	998.4	–9.25	–0.6	75.2	91.5	41	59
115a	115a-G55	47.69	0.77	17.56	1.85	9.71	0.31	5.74	11.38	1.56	0.07	0.08	3.28	1003.6	–9.17	–0.6	75.4	91.4	34	66
115a	115a-G57	47.75	0.79	17.38	1.98	9.84	0.18	5.88	11.13	1.73	0.07	0.16	3.11	1012.6	–9.03	–0.5	75.6	88.9	44	56
6636/gp-15	G104-1	55.53	0.83	15.97	1.53	7.94	0.29	3.64	7.97	2.98	0.15	0.20	2.97	979.6	–9.54	–0.6	69.8	71.9	25	75
6636/gp-15	G105-1	54.91	0.87	16.19	1.62	8.32	0.15	3.67	8.05	2.70	0.15	0.20	3.16	976.7	–9.59	–0.6	68.8	75.3	23	77
6636/gp-15	G105-2	54.32	0.81	16.06	1.77	8.63	0.36	3.81	8.24	2.60	0.23	0.13	3.04	979.6	–9.54	–0.6	68.6	76.0	25	75
6636/gp-15	G106-1	52.46	1.00	15.83	2.32	9.61	0.36	4.61	7.66	2.69	0.09	0.31	3.06	971.7	–9.67	–0.6	69.3	74.4	27	73
6636/gp-15	G111-1	54.66	0.87	16.09	1.75	8.77	0.33	4.01	7.60	2.54	0.20	0.13	3.06	982.2	–9.50	–0.6	69.0	76.7	25	75
6636/gp-18	G-114-1	49.38	0.81	17.34	1.33	8.60	0.06	5.57	12.15	1.38	0.11	0.14	3.13	990.5	–9.37	–0.6	76.9	93.2	26	74
6636/gp-18	G117-2	48.62	0.75	17.47	1.48	8.94	0.31	5.72	11.52	1.56	0.11	0.24	3.30	999.1	–9.24	–0.6	76.8	91.3	24	76
6636/gp-18	G-118-1	49.12	0.67	17.97	1.33	9.02	0.17	5.98	11.08	1.20	0.16	0.17	3.14	1010.0	–9.07	–0.5	77.2	97.1	24	76

Note: *T* is the temperature of cotectic crystallization of olivine and plagioclase; $\log f_{O_2}$ is the oxygen fugacity; dNNO is the deviation of f_{O_2} from the NNO buffer in logarithmic units; *Fo* is the forsterite mole fraction of olivine crystallizing from the melt; *An* is the anorthite mole fraction of plagioclase crystallizing from the melt; *Ol* is the content of olivine in the cumulate; and *Pl* is the content of plagioclase in the cumulate. The analyses were recalculated to totals of 100%.

whereas allivalites usually occur in more silicic rocks. Solid-state deformation textures and banded structures observed in some allivalites could not develop in crystal clots immersed in a melt.

Volynets et al. (1978) supposed that allivalites were formed on the walls of magma conduits and are fragments of a peculiar vent facies. Some allivalites of pegmatoid structure could probably form in such a way. However, given the high temperature gradients and rapid mineral growth, distinct mineral zoning and considerable variation in mineral composition within a single sample should be expected.

Frolova and Dril' (1993) and Frolova et al. (2000) proposed a cumulate origin for allivalites with the fractionation of olivine–plagioclase cumulates during early stages of evolution of low-potassium island-arc tholeiites. These authors suggested the existence of a common high-alumina and low-potassium primary melt, which produced all of the volcanic series containing allivalites. The hypothesis of the cumulate nature of allivalites seems to be more plausible than the other aforementioned hypotheses. It is supported by petrographic observations and mass balance calculations (Frolova and Dril', 1993; Frolova et al., 2000; this study). The obtained new comprehensive data on a wide range of melt and mineral compositions and conditions under which allivalites were formed can be used to quantitatively evaluate the hypothesis of their cumulate origin.

Relationships of the Compositions of Allivalites, Melt Inclusions, Groundmass Glasses, and Volcanic Rocks

The compositions of melts from the inclusions plot on the same trends as the intercumuls material and groundmass glasses (Fig. 10), at its least differentiated part (relatively high contents of MgO, FeO_{tot}, CaO, and Al_2O_3 and low SiO_2 and Na_2O). This indicates that the cumulate layer retained portions of the melts from which the minerals of allivalites crystallized, i.e., the allivalite nodules could not be fragments of completely crystallized intrusive rocks.

In order to check the cumulate nature of allivalites, we performed mass balance calculations (Table 9), which demonstrated that cumulates of the allivalite composition could be produced from the initial melt with the formation of a residual melt corresponding to low-potassium tholeiites. The calculations were carried out for the average compositions of allivalites, initial melts, and fine-grained groundmass, which was considered as a proxy for the residual melt after the crystallization and accumulation of allivalite minerals. We used 56 bulk-rock analyses of allivalites from the literature, 17 compositions of intercumulus materials, and 31 recalculated compositions of melt inclusions in olivine from allivalites.

The proportions of crystallized material and residual melts vary significantly among the volcanoes. For instance, the fraction of cumulates relative to the initial melt may be up to 32% for Golovnin Volcano, 43% for Zavaritskii Volcano, 35% for Ksudach Volcano, and 46% for Kudryavyi Volcano (Table 9).

The mass balance was calculated between the primary melt (estimated from melt inclusions in olivine) on the one hand and minerals crystallizing in the allivalites (olivine, plagioclase, clinopyroxene, and titanomagnetite) and initial melt (interstitial material) on the other hand. This balance reflects the degree of melt fractionation during allivalite cumulation. The following proportions were calculated for various volcanoes: 78 wt % melt + 3 wt % olivine + 15 wt % plagioclase + 2 wt % clinopyroxene + 2 wt % titanomagnetite for Golovnin Volcano, 71 wt % residual melt + 1 wt % olivine + 25 wt % plagioclase + 5 wt % clinopyroxene for Ksudach Volcano, and 59 wt % melt + 9 wt % olivine + 29 wt % plagioclase + 8 wt % clinopyroxene + 2 wt % titanomagnetite for Kudryavyi Volcano (Table 10).

The bulk compositions of allivalites are systematically different from the compositions of melts and show lower contents of SiO_2, K_2O, Na_2O, and TiO_2 and higher Al_2O_3, CaO, and MgO (Fig. 10). Some allivalite compositions are similar to the melts with respect to all components. These rocks are rich in clinopyroxene and/or contain considerable amounts of groundmass glass and are transitional between allivalites, gabbroid-type enclaves, and porphyritic basalts. The difference in FeO and TiO_2 contents between the bulk-rock compositions of allivalites and the analyses of melts reported here could be related to the separation of titanomagnetite during the formation of cumulate layers.

Using the Petrolog III program (Plechov and Danyushhevskii, 2006), fractional crystallization of olivine and plagioclase from melts trapped in the most magnesian olivines was modeled for each of the volcanoes studied. The compositions of olivine and plagioclase were calculated by the models of Danyushevsky (2001) and Pletchov and Gerya (1998), respectively. The calculations were stopped when the composition of the most iron-rich olivine observed in allivalites from the given volcano was attained. For the samples from Ksudach Volcano, we obtained 35% of cumulate consisting of 84.4 wt % plagioclase ($An_{91.2}$) and 15.6 wt % olivine ($Fo_{78.6}$). The range of olivine composition Fo_{79-74} was used for Golovnin Volcano, because allivalites with a more ferriferous olivine described in this volcano contain significant amounts of clinopyroxene. The calculations yielded 24% of cumulate consisting of 81.7 wt % plagioclase ($An_{94.7}$) and 18.3 wt % olivine ($Fo_{75.7}$). The considerable variations in mineral proportions in the allivalites and the observed banded structures in some samples can be explained by the accumulation of rhythmically banded olivine–anorthite cumulates.

Table 9. Mass balance relations between the parental melt of allivalites ('melt'), bulk compositions of allivalites ('allivalite'), and compositions of intercumulus material ('intercumulus')

Phase	Number of analyses	Fraction of phase	SiO_2	TiO_2	Al_2O_3	FeO_{tot}	MnO	MgO	CaO	Na_2O	K_2O	Total
Ksudach Volcano												
Melt	31	**1**	50.35	0.83	16.89	9.93	0.25	6.67	12.74	2.05	0.29	100.00
Intercumulus	11	**0.65**	49.95	0.94	13.94	14.99	0.30	8.16	8.94	2.45	0.32	100.00
Allivalite	17	**0.35**	42.91	0.29	22.30	7.15	0.09	11.84	14.53	0.78	0.10	100.00
Calculated composition			47.51	0.71	16.85	12.27	0.23	9.44	10.88	1.87	0.24	100.00
Squared deviation			8.06	0.01	0.00	5.49	0.00	7.63	3.46	0.03	0.00	**24.70**
Zavaritskii Volcano												
Melt	12	**1**	47.02	0.81	18.83	13.09	0.24	8.36	10.01	1.43	0.21	100.00
Intercumulus	3	**0.57**	53.11	0.84	16.23	10.62	0.22	4.31	11.55	2.86	0.25	100.00
Allivalite	11	**0.43**	42.88	0.15	23.56	7.27	0.11	10.87	14.54	0.61	0.02	100.00
Calculated composition			48.68	0.54	19.40	9.17	0.18	7.15	12.84	1.88	0.15	100.00
Squared deviation			2.77	0.07	0.32	15.37	0.00	1.46	8.05	0.21	0.00	**28.26**
Kudryavyi Volcano												
Melt	7	**1**	49.98	0.78	17.20	11.61	0.30	7.07	10.77	2.03	0.26	100.00
Intercumulus	1	**0.54**	56.64	1.69	15.41	11.36	0.25	2.88	8.15	3.16	0.46	100.00
Allivalite	5	**0.46**	42.72	0.83	22.70	10.13	0.12	9.07	13.58	0.73	0.12	100.00
Calculated composition			50.20	1.29	18.78	10.79	0.19	5.74	10.66	2.04	0.30	100.00
Squared deviation			0.05	0.26	2.49	0.68	0.01	1.76	0.01	0.00	0.00	**5.26**
Golovnin Volcano												
Melt	5	**1**	48.87	0.73	17.28	12.87	0.28	7.11	11.09	1.68	0.09	100.00
Intercumulus	2	**0.68**	51.28	0.81	15.50	13.01	0.25	8.01	9.47	1.60	0.07	100.00
Allivalite	1	**0.32**	43.67	1.19	17.20	16.04	0.19	6.41	13.92	1.20	0.16	100.00
Calculated composition			48.86	0.93	16.04	13.98	0.23	7.50	10.88	1.48	0.10	100.00
Squared deviation			0.00	0.04	1.53	1.23	0.00	0.15	0.04	0.04	0.00	**3.04**

Note: The “Calculated composition” is the sum of the initial compositions of allivalite and intercumulus in chosen proportions (shown in bold) determined by minimizing the sum of the squared differences of component contents between the measured and calculated melt compositions (shown in bold).

Origin of the Structural Diversity of Allivalites

Many of the allivalite samples show signs of recrystallization. The most spectacular in this respect are concentrically zoned allivalites from Kudryavyi Volcano (Figs. 2b, 2d, 2f), which consist of a conspicuous coarse-grained central zone surrounded by a finer grained plagioclase–olivine aggregate. The compositions of minerals from the central and marginal zones of these samples are identical, and the differences are restricted to textural and structural characteristics. In our opinion, such a concentric zoning could be formed by the recrystallization of the outer zone of a cumulate fragment after its entrainment by the magma which transported it to the surface. During the same stage, the cumulate fragments could acquire spherical shapes. This suggestion is supported by the lack of melt inclusions in minerals from the recrystallized marginal zones of the allivalites, whereas olivine and plagioclase grains from the central zones contain large primary partly crystallized melt inclusions. The concentrically

Table 10. Mass balance relations for the parental melts of allivalites ('melt'), their major minerals, and intercumulus materials ('intercumulus')

Mineral or melt	Fraction of mineral or melt	SiO_2	TiO_2	Al_2O_3	FeO_{tot}	MnO	MgO	CaO	Na_2O	K_2O	Total
Golovnin Volcano											
Olivine	**0.03**	38.60	0.03	0.01	22.01	0.37	38.65	0.16	0.14	0.02	100.00
Plagioclase	**0.15**	43.20	0.02	36.00	0.55	0.00	0.01	19.77	0.43	0.00	100.00
Titanomagnetite	**0.02**	0.20	7.66	4.94	83.60	0.24	3.23	0.00	0.12	0.01	100.00
Clinopyroxene	**0.02**	51.31	0.35	3.12	7.70	0.17	15.38	21.82	0.14	0.01	100.00
Intercumulus	**0.78**	51.28	0.81	15.50	13.01	0.25	8.01	9.47	1.60	0.07	100.00
Melt	**1**	48.87	0.73	17.28	12.87	0.28	7.11	11.09	1.68	0.09	100.00
Calculated composition		48.64	0.80	17.57	12.74	0.22	7.85	10.82	1.32	0.05	
Squared deviation		0.05	0.00	0.08	0.02	0.00	0.54	0.07	0.13	0.00	**0.90**
Kudryavyi Volcano											
Olivine	**0.09**	38.65	0.02	0.01	19.03	0.29	41.69	0.21	0.09	0.01	100.00
Plagioclase	**0.22**	44.69	0.01	34.53	0.70	0.04	0.07	19.27	0.67	0.01	100.00
Titanomagnetite	**0.02**	0.22	7.77	4.06	85.41	0.15	2.07	0.02	0.23	0.07	100.00
Clinopyroxene	**0.08**	46.72	1.55	6.05	13.33	0.24	11.52	20.26	0.31	0.02	100.00
Intercumulus	**0.59**	56.64	1.69	15.41	11.36	0.25	2.88	8.15	3.16	0.46	100.00
Melt	**1**	49.98	0.78	17.20	11.61	0.30	7.07	10.77	2.03	0.26	100.00
Calculated composition		50.37	1.28	17.18	11.45	0.21	6.59	10.61	2.04	0.28	
Squared deviation		0.15	0.25	0.00	0.03	0.01	0.23	0.03	0.00	0.00	**0.70**
Ksudach Volcano											
Olivine	**0.01**	39.04	0.03	0.01	18.57	0.35	41.60	0.21	0.18	0.02	100.00
Plagioclase	**0.25**	43.62	0.02	35.65	0.60	0.05	0.06	19.37	0.62	0.01	100.00
Titanomagnetite	**0.05**	48.89	1.00	4.77	10.19	0.24	13.35	21.29	0.25	0.01	100.00
Clinopyroxene	**–0.02**	0.60	7.86	3.98	85.14	0.58	1.42	0.21	0.21	0.00	100.00
Intercumulus	**0.71**	49.95	0.94	13.94	14.99	0.30	8.16	8.94	2.45	0.32	100.00
Melt	**1**	49.93	0.64	19.21	9.62	0.39	6.20	12.00	1.80	0.20	100.00
Calculated composition		49.31	0.54	19.05	9.55	0.23	6.88	12.31	1.90	0.23	
Squared deviation		0.39	0.01	0.03	0.01	0.03	0.45	0.10	0.01	0.00	**1.02**

zoned allivalites of Kudryavyi Volcano are surrounded by an andesitic mantle (60–62 wt % SiO_2) containing large phenocrysts of clinopyroxene, magnetite, and zoned labradorite, which are partly replaced by a cryptocrystalline aggregate (Fig. 2l) containing up to 90–95 wt % SiO_2. The groundmass is made up of plagioclase, pyroxene, and magnetite microlites. The structural diversity of allivalites described above can be explained by the following sequence of events: (1) accumulation of cumulate layers in the magma chamber with possible formation of banded structures; (2) deformations of the cumulate layer with possible formation of deformation textures and deformation twins of plagioclase; (3) shattering of the cumulate layer to separate blocks by the magma invading the chamber; (4) entrainment of individual allivalite blocks by magma convection, owing to which some of them may be partly recrystallized and acquire spherical out-lines; and (5) transportation of allivalites to the surface during large explosive eruptions.

Crystallization Conditions and Compositions of Initial Melts

Temperatures of 970–1080°C were calculated for the formation of allivalites via simultaneous crystallization of olivine and plagioclase from a melt (Tables 7, 8). The crystallization occurred under relatively oxidizing conditions at f_{O_2} values approximately one order of magnitude above the Ni–NiO buffer equilibrium (ΔNNO = +1), which was estimated above on the basis of chrome spinel composition (Fig. 5). The available data do not allow us to precisely determine the total pressure of crystallization, but it was presumably about 1 kbar, which corresponds to the conditions of melt saturation with a water-dominated fluid at the measured melt H_2O content (3.0–3.5 wt %) (Moore et al., 1998).

The highest temperatures of 1050–1085°C were obtained for the melts of allivalites from Zavaritskii Volcano (MgO ~ 7.3 wt %), and the lowest, for allivalites with relatively Fe-rich olivine (*Fo* < 76 mol %) from Ksudach (970–985°C) and Golovnin volcanoes (MgO ~ 4–5 wt %, 990–1020°C). The anorthite mole fraction of plagioclase in allivalites from a particular volcanic center (for instance, Golovnin or Ksudach) decreases with decreasing temperature and MgO content in accordance with the expected effect of the simultaneous crystallization of plagioclase and olivine. However, there is no general correlation between the composition of plagioclase and MgO content in the initial melts of allivalites. The most calcic plagioclase occurs in Golovnin Volcano; intermediate compositions were observed in Ksudach, Zavaritskii, and Kudryavyi volcanoes; and the least calcic plagioclase was reported from Il'inskii Volcano. The reasons for the variations in plagioclase composition are not fully understood and could be related to both systematic variations in the initial contents of major elements in the melts (Si, Al, Ca, and Na) and variable amounts of H_2O (Panajaswatwong et al., 1995; Pletchov and Gerya, 1998). The elucidation of the nature of these variations is a topic for future research.

The average compositions of initial melts for the samples studied are strongly variable. All of the melts show a strong positive correlation between the contents of MgO (4.2–7.3 wt %) and Al_2O_3 (16.8–19.3 wt %) and negative correlations between MgO, SiO_2 (47.2–55.0 wt %), and Na_2O (1.4–2.8 wt %). The contents of FeO (9.5–12.5 wt %) and CaO (8.4–13.1 wt %) show no systematic variations with MgO. For individual volcanoes, the FeO content of melt remains approximately constant, while CaO decreases with decreasing MgO. In individual volcanic centers, the contents of TiO_2 and K_2O increase with decreasing MgO. The melts of Golovnin Volcano show the maximum TiO_2 and K_2O depletion. Low K_2O contents are also characteristic of Il'inskii Volcano.

The compositions of the initial melts of allivalites are closely similar to those of basalts and basaltic andesites of the low-K series of Kamchatka and the Kuril Islands, which indicates their certain genetic relation and formation through the evolution of common parental magmas, whose compositions were somewhat different for different volcanoes. The compositions of the initial melts of allivalites evolve toward SiO_2 enrichment and MgO depletion and can be parental for typical andesites (Fig. 10).

Mass balance calculations for the allivalite samples from Golovnin and Ksudach volcanoes showed that the liquid lines of descent can be explained by the simultaneous crystallization of olivine, plagioclase, pyroxene, and magnetite in the proportion 4 : 20 : 12 : 3, which is close to the observed relative abundances of the minerals in the allivalites. The modeling of fractional crystallization showed the possibility of formation of cumulates with similar proportions of olivine and plagioclase. Relative to the initial mass of primitive melt, the amount of the cumulate is 22–32% for Golovnin Volcano and 29–35% for Ksudach Volcano.

Thus, it can be concluded that allivalites are products of the early crystallization of olivine, plagioclase, magnetite, and clinopyroxene from relatively primitive (6.0–7.5 wt % MgO) initial magmas, which resulted in the formation of typical low-K andesite series of Kamchatka and the Kuril Islands.

Allivalites are formed by the crystallization, separation, and deformation of olivine–plagioclase cumulates in magma chambers followed by the destruction of the cumulate layers and transportation of the resulting nodules by pyroclastic surges of silicic composition. A considerable time period is needed for the sequential occurrence of these processes. As was noted above, all of the findings of allivalites were restricted to long-lived volcanic centers, whose magma chambers could operate for tens of thousand years. Amma-Miyasaka and Nakagawa (2002) attempted to estimate the time assuming a diffusion-related obliteration of zoning in plagioclases. They estimated that zoning can be obliterated over a distance of 100 μm in 10 kyr. As the unzoned plagioclase grains from the allivalite samples studied by us are up to 15 mm in size, the time necessary to obliterate the primary zoning is evidently greater than the life-time of even long-lived volcanic centers. Thus, the plagioclases were inherently unzoned, which requires large volumes of magmatic melt and stable conditions in the magma chamber.

Mass balance and thermodynamic calculations showed that clinopyroxene had to cocrystallize with olivine and plagioclase. However, clinopyroxene is rare in allivalites, which indicates efficient separation of clinopyroxene during the formation of cumulate layers. The mechanisms and dynamics of this separation are not clear. Ermakov and Pecherskii (1989) distinguished a gabbro–allivalite association of cognate enclaves with variable mineral compositions, which were combined on the basis of the presence of anorthite. Perhaps, the investigations of other rocks of this association will provide a better insight into the formation of cumulate layers. Another unsolved question is why the conditions of allivalite formation were attained only in the volcanic centers of front arc areas. It is conceivable that this is related to the specific features of the fractionation of low-K island-arc series, which are confined to the volcanic front. However, the formation of low-K melts and the dynamics of their fractionation require further investigations.

CONCLUSIONS

(1) Silica-poor anorthite–olivine enclaves are fragments of cumulates of low-potassium and water-rich (3.0–3.5 wt % H_2O) primary basaltic magmas. The accumulation occurred in large-volume magma chambers under relatively quiet conditions. In some cases, these rocks experienced partial recrystallization either directly in the cumulate layer or during their transportation toward the surface, which is responsible for the observed structural diversity of allivalites.

(2) A quantitative method was proposed for the determination of the compositions of initial melts of olivine–plagioclase cumulate rocks on the basis of the compositions of partly homogenized melt inclusions and the contents of magmatic H_2O in them. Using this method, the initial compositions of parental allivalite melts were reconstructed. Their crystallization occurred at temperatures of 970–1080°C under relatively oxidizing conditions (ΔNNO = +1) and close to saturation with an aqueous fluid at pressures of ~1 kbar.

(3) The degree of fractionation of primary melts during the formation of cumulate layers of allivalite compositions varies from 22 to 46%. Perhaps, the range of crystallization recorded in the compositions of allivalites and melt inclusions corresponds to the early stage of evolution of the parental low-K magmas. Their subsequent evolution produced the strongly differentiated series of low-K basalts, andesites, and dacites of Kamchatka and the Kuril Islands.

ACKNOWLEDGMENTS

The authors are grateful to L.P. Anikin, S. Chirkov (Institute of Volcanology, Far East Division, Russian Academy of Sciences), V.L. Syvorotkin (Moscow State University), and I.N. Bindeman (University of Oregon, Eugene, USA), who kindly provided allivalite samples for our investigations, and I.P. Solovova (Institute of Geology of Ore Deposits, Petrography, Mineralogy, and Geochemistry, Russian Academy of Sciences) for constructive comments. This study was financially supported by Russian President's Program for the Support of Leading Scientific Schools (grant no. 5338.2006.5, supervised by L.L. Perchuk), Royal Society, and Russian Foundation for Basic Research (project nos. 05-01-02901-YaF-a, 06-05-64873, and 07-05-00807).

REFERENCES

1. *Active Volcanoes of Kamchatka*, Ed. by S. A. Fedotov and Yu. P. Masurenkov (Nauka, Moscow, 1991), Vol. 2 [in Russian].
2. R. R. Al'meev and A. A. Ariskin, "Mineral–Melt Equilibria in a Hydrous Basaltic System: Computer Modeling," Geokhimiya, No. 7, 624–636 (1996) [Geochem. Int. **34**, 563–573 (1996)].
3. M. Amma-Miyasaka and M. Nakagawa, "Origin of Anorthite and Olivine Megacrysts in Island-Arc Tholeiites: Petrological Study of 1940 and 1962 Ejecta from Miyake-jima Volcano, Izu–Mariana Arc," J. Volcanol. Geotherm. Res. **117**, 263–283 (2002).
4. V. V. Anan'ev and G. D. Shnyrev, "Garnet in Melt Inclusions from Olivine of *Ol–An* Segregations (Ksudach Volcano, Kamchatka)," Dokl. Akad. Nauk SSSR **274**, 402–406 (1984).
5. J. Anderson and D. R. Smith, "The Effect of Temperature and Oxygen Fugacity on Al-in-Hornblende Barometry," Am. Mineral. **80**, 549–559 (1995).
6. R. J. Arculus and K. J. A. Wills, "The Petrology of Plutonic Blocks and Inclusions from the Lesser Antilles Island Arc," J. Petrol. **21**, 743–799 (1980).
7. A. A. Ariskin, G. S. Barmina, M. Ya. Frenkel, and R. L. Nielsen, "COMAGMAT: A Fortran Program to Model Magma Differentiation Processes," Comp. Geosci. **19**, 1155–1170 (1993).
8. J. C. Bailey, T. I. Frolova, and I. A. Burikova, "Mineralogy, Geochemistry and Petrogenesis of Kurile Island-Arc Basalts," Contrib. Mineral. Petrol. **102**, 265–280 (1987).
9. C. Ballhaus, R. Berry, and D. Green, "High Pressure Experimental Calibration of the Olivine–Orthopyroxene–Spinel Oxygen Geobarometer: Implications for the Oxidation State of the Upper Mantle," Contrib. Mineral. Petrol. **107**, 27–40 (1991).
10. G. E. Bogoyavlenskaya and E. N. Erlikh, "Feldspathic Basic Inclusions in the Felsic Pyroclastic Rocks of Modern Volcanoes," in *Xenoliths and Cognate Inclusions* (Nauka, Moscow, 1969), pp. 64–67 [in Russian].
11. C. H. Chen, "Significance of Ultrabasic Inclusions in Tatun Volcano Group, Northern Taiwan," J. Geol. Soc. China **21**, 80–91 (1978).
12. L. V. Danyushevsky, "The Effect of Small Amounts of H_2O on Crystallisation of Mid-Ocean Ridge and Backarc Basin Magmas," J. Volcanol. Geotherm. Res. **110**, 265–280 (2001).
13. L. V. Danyushevsky, F. N. Della-Pasqua, and S. Sokolov, "Re-Equilibration of Melt Inclusions Trapped by Magnesian Olivine Phenocrysts from Subduction-Related Magmas: Petrological Implications," Contrib. Mineral. Petrol. **138**, 68–83 (2000).
14. L. V. Danyushevsky, A. W. McNeill, and A. V. Sobolev, "Experimental and Petrological Studies of Melt Inclusions in Phenocrysts from Mantle-Derived Magmas: An Overview of Techniques, Advantages and Complications," Chem. Geol. **183**, 5–24 (2002a).

15. L. V. Danyushevsky, S. Sokolov, and T. Falloon, "Melt Inclusions in Phenocrysts: Using Diffusive Re-Equlibration to Determine the Cooling History of a Crystal, with Implications for the Origin of Olivine-Phyric Volcanic Rocks," J. Petrol. **43**, 1651–1671 (2002b).
16. S. I. Dril', Candidate's Dissertation in Geology and Mineralogy (Moscow, 1988).
17. Yu. M. Dubik, "Xenoliths and Ultrabasic Inclusions in the Lavas of Ksudach Volcano (Southern Kamchatka)," in *Volcanism, Hydrothermal Systems, and Earth's Interior* (Petropavlovsk-Kamchatskii, 1969), pp. 44–54 [in Russian].
18. V. A. Ermakov and D. M. Pecherskii, "Nature of Gabbroid Inclusions from the Young Lavas of the Kuril Islands," Tikhookean. Geol., No. 4, 45–55 (1989).
19. V. A. Ermakov, O. N. Volynets, and A. V. Koloskov, "Inclusions in Volcanic Rocks," in *Petrology and Geochemistry of Island Arcs and Marginal Seas* (Nauka, Moscow, 1987), pp. 293–312 [in Russian].
20. C. E. Ford, D. G. Russel, J. A. Graven, "Olivine–Liquid Equilibria: Temperature, Pressure and Composition Dependence of the Crystal/Liquid Cation Partition Coefficients for Mg, Fe^{2+}, Ca and Mn," J. Petrol. **24**, 256–265 (1983).
21. T. I. Frolova and S. A. Dril', "Andesite Volcanism of Island Arcs and Its Geological Significance," Tikhookean. Geol., No. 3, 3–14 (1993).
22. T. I. Frolova, J. Bailey, I. A. Burikova, and S. I. Dril', "On Genetic Relations between Low-Silica Olivine–Anorthite Inclusions and their Host Rocks from the Kuril Island Arc," Tikhookean. Geol., No. 5, 27–35 (1988).
23. T. I. Frolova, I. A. Burikova, S. I. Dril', et al., "Nature of Low-Silica Olivine–Anorthite Inclusions and Conditions of Their Formation," Tikhookean. Geol., No. 6, 85–95 (1989).
24. T. I. Frolova, P. Yu. Plechov, P. L. Tikhomirov, and S. V. Churakov, "Melt Inclusions in Minerals of Allivalites of the Kuril–Kamchatka Island Arc," Geokhimiya, No. 4, 336–346 (2000) [Geochem. Int. **39**, 336–346 (2001)].
25. L. L. Gee and R. O. Sack, "Experimental Petrology of Melilite Nephelinites," J. Petrol. **29**, 1233–1255 (1988).
26. G. S. Gorshkov, *Volcanism and the Upper Mantle. Investigations in the Kurile Island Arc* (Plenum, New York–London, 1970).
27. E. N. Grib, "Petrology of the Products of the Eruption of 2–3 January 1996 in the Akademii Nauk Caldera," Vulkanol. Seismol., No. 5, 71–96 (1997).
28. T. Grove and M. B. Baker, "Phase Equilibrium Controls on the Tholeiitic versus Calc-Alkaline Differentiation Trends," J. Geophys. Res. **89**, 3253–3274 (1984).
29. A. Harker, *The natural history of igneous rocks* (Methuen, London, 1909).
30. T. Ishikawa, "Petrological Significance of Large Anorthite Crystals Included in Some Pyroxene Andesites and Basalts in Japan," J. Fac. Sci. Hokkaido Univ. Ser. 4. Geol. Mineral. **7**, 339–354 (1951).
31. B. E. Leake, A. R. Woolley, C. E. S. Arps, et al., "Nomenclature of Amphiboles: Report of the Subcommittee on Amphiboles of the International Mineralogical Association, Commission on New Minerals and Mineral Names," Can. Mineral. **35**, 219–246 (1997).
32. K. L. Lundgaard, B. Robins, C. Tegner, and J. R. Wilson, "Formation of Hybrid Cumulates: Melatroctolites in Intrusion 4 of the Honningsvåg Intrusive Suite, Northern Norway," Lithos **61**, 1–19 (2002).
33. Yu. P. Masurenkov, "Problem of Inclusions and Resources of Volcanic Petrology," Byull. Vulkanol. Stantsii, No. 50, 10–18 (1974).
34. G. Moore, T. Vennemann, and I. S. E. Carmichael, "An Empirical Model for the Solubility of H_2O in Magmas to 3 Kilobars," Am. Mineral. **83**, 36–42 (1998).
35. V. F. Ostapenko, V. I. Fedorchenko, and V. N. Shilov, "Pumices, Ignimbrites and Rhyolites from the Great Kuril Arc," Bull. Volcanol. **30**, 81–92 (1967).
36. Y. Panajaswatwong, L. V. Danyushevsky, A. J. Crawford, and K. L. Harris, "An Experimental Study of the Effects of Melt Composition on Plagioclase–Melt Equilibria at 5 and 10 kbar: Implications for the Origin of Magmatic High-*An* Plagioclase," Contrib. Mineral. Petrol. **118**, 420–432 (1995).
37. B. I. Piip, "Field Geological Observations in Southern Kamchatka," Tr. Kamchatskoi Vulkanol. St. (Akad. Nauk SSSR, Moscow, 1947), No. 3, pp. 89–136 [in Russian].
38. B. N. Piskunov, "Classification of Quaternary Volcanic Series and Lateral Petrochemical Zoning of the Kuril–Kamchatka Arc," in *Volcanism of the Kuril–Kamchatka Region and Sakhalin Island*, Tr. Sakh. Kompl. Nauchn.-Issled. Inst., No. 48, 17–33 (1976).
39. P. Yu. Pletchov and L. V. Danyushevskii, "RETROLOG III. Modeling of Equilibrium and Fractional Crystallization," in Proceeding of ESMPG (2006), Vestn Otd. Nauk Zemle, No. 1, 24 (2006).
40. P. Yu. Pletchov and T. V. Gerya, "Effect of H_2O on Plagioclase–Melt Equilibrium," Experiment in Geosciences **7** (2), 7–9 (1998).
41. E. I. Popolitov and O. N. Volynets, *Geochemical Characteristics of the Quaternary Volcanism of the Kuril–Kamchatka Island Arc and Some Petrogenetic Problems* (Nauka, Novosibirsk, 1981) [in Russian].
42. M. V. Portnyagin, N. L. Mironov, S. V. Matveev, and P. Yu. Plechov, "Petrology of Avachites, High-Magnesian Basalts of Avachinsky Volcano, Kamchatka: II. Melt Inclusions in Olivine," Petrologiya **13**, 358–388 (2005) [Petrology **13**, 322–351 (2005)].
43. V. S. Prikhod'ko, A. F. Bekhtol'd, and I. M. Romanenko, "Cr-Spinellids of Allivalite Inclusions and Their Petrological Significance," Dokl. Akad. Nauk SSSR **235**, 918–920 (1977).
44. R. I. Rodionova and V. I. Fedorchenko, "Xenoliths in the Lavas of the Kuril Islands and Some Problems of the Deep Geology of This Region," in *Volcanism and the Earth's Interiors* (Nauka, Moscow, 1971), pp. 141–147 [in Russian].
45. R. O. Sack and I. S. E. Carmichael, "$Fe^{2+} = Mg^{2+}$ and $TiAl_2 = MgSi_2$ Exchange Reactions between Clinopyroxenes and Silicate Melt," Contrib. Mineral. Petrol. **85**, 103–115 (1984).
46. O. B. Selyangin, "Cognate Inclusions and Possibility of the Reconstruction of the Mechanism of Magma Differentiation in Volcanic Edifices," Byull. Vulkanol. St., No. 50, 45–52 (1974).

47. O. B. Selyangin, "On the Formation Temperatures of Some Crystalline Inclusions in the Recent Volcanics of Kamchatka," Byull. Vulkanol. St., No. 51, 74–76 (1975).

48. O. B. Selyangin, *Petrogenesis of the Basalt–Dacite Series with Applications to the Evolution of Volcanic Structures* (Nauka, Moscow, 1987) [in Russian].

49. V. S. Sheimovich, "Ksudach Volcano in August 1963," Byull. Vulkanol. St., No. 41, 25–28 (1966).

50. T. Simkin and J. V. Smith, "Minor-Element Distribution in Olivine," J. Geol. **78**, 304–325 (1970).

51. A. V. Sobolev, "Melt Inclusions in Minerals as a Source of Principle Petrological Information," Petrologiya **4**, 228–239 (1996) [Petrology **4**, 209–220 (1996)].

52. A. V. Sobolev, L. V. Dmitriev, V. L. Barsukov, et al., "The Formation Conditions of High Magnesium Olivines from the Monomineral Fraction of Luna-24 Regolith," 11th Lunar Planet. Sci. Conf. 105–116 (1980).

53. V. L. Syvorotkin, "Crustal Volcanics of the Kuril–Kamchatka Arc," Obshch. Reg. Geol., Geol. Morei Okean., Geol. Kartir: Obzor. Inform., Issue 5 (1996).

54. O. N. Volynets, S. A. Shcheka, and Yu. M. Dubik, "Olivine–Anorthite Inclusions in the Volcanoes of Kamchatka and Kurils," *Inclusions in the Volcanic Rocks of the Kuril–Kamchatka Island Arc*, Ed. by B. G. Lutts, K. N. Rudich, and V. A. Ermakov (Nauka, Moscow, 1978), pp. 124–166 [in Russian].

55. S. E. Zharinov, "Petrochemical Variations of Island Arc Andesites (Kurile Island Arc)," J. Geophys. Res. **93**, 14828–14834 (1988).